physics

MDPI

Review

Novel Cs_2HfCl_6 Crystal Scintillator: Recent Progress and Perspectives

Serge Nagorny [1,2]

[1] Department of Physics, Engineering Physics and Astronomy, Queen's University, Kingston, ON K7L 3N6, Canada; sn65@queensu.ca
[2] Arthur B. McDonald Canadian Astroparticle Physics Research Institute, Kingston, ON K7L 3N6, Canada

Abstract: Recent progress in Cs_2HfCl_6 (CHC) crystal production achieved within the last five years is presented. Various aspects have been analyzed, including the chemical purity of raw materials, purification methods, optimization of the growth and thermal conditions, crystal characterization, defect structure, and internal radioactive background. Large volume, crack-free, and high quality CHC crystals with an ultimate scintillating performance were produced as a result of such extensive research and development (R & D) program. For example, the CHC crystal sample with dimensions $\varnothing 23 \times 30$ mm^3 demonstrates energy resolution of 3.2% FWHM at 662 keV, the relative light output at the level of 30,000 ph/MeV and excellent linearity down to 20 keV. Additionally, this material exhibits excellent pulse shape discrimination ability and low internal background of less than 1 Bq/kg. Furthermore, attempts to produce a high quality CHC crystal resulted in research on this material optimization by constitution of either alkali ions (Cs to Tl), or main element (Hf to Zr), or halogen ions (Cl to Br, I, or their mixture in different ratio), as well as doping with various active ions (Te^{4+}, Ce^{3+}, Eu^{3+}, etc.). This leads to a range of new established scintillating materials, such as Tl_2HfCl_6, Tl_2ZrCl_6, $Cs_2HfCl_4Br_2$, $Cs_2HfCl_3Br_3$, Cs_2ZrCl_6, and Cs_2HfI_6. To exploit the whole potential of these compounds, detailed studies of the material's fundamental properties, and understanding of the variety of the luminescence mechanisms are required. This will help to understand the origin of the high light yield and possible paths to further extend it. Perspectives of CHC crystals and related materials as detectors for rare nuclear processes are also discussed.

Keywords: Cs_2HfCl_6 crystals; scintillator; purification; crystal growth; light yield; energy resolution; defect structure; quenching factor; gamma-spectroscopy; rare decays

Citation: Nagorny, S. Novel Cs_2HfCl_6 Crystal Scintillator: Recent Progress and Perspectives. *Physics* **2021**, *3*, 320–351. https://doi.org/10.3390/physics3020023

Received: 6 February 2021
Accepted: 6 May 2021
Published: 13 May 2021

1. Introduction

The study of rare nuclear processes (rare alpha and beta decays, neutrinoless double beta decay, or dark matter (DM) particle direct detection) is an active field of research with steady improvements utilizing more and more sensitive detectors. Experimental information on rare decays supports the understanding of nuclear structure, has applications in a variety of fields, e.g., nuclear chronometers, and is relevant as long-lived backgrounds in other rare events searches. As regards neutrinoless double beta decay, it can shed light on fundamental mechanism beyond the standard model of particle physics. Many experiments exploiting various detector techniques aiming to search for these elusive nuclear processes with half-lives longer than age of the universe (on the scale of 10^{14} y) were proposed and realized within last 20 years. The highest sensitivity was achieved using "source = detector" experimental approach, where the isotope of interest is embedded into the detector material. A major advantage of the "source = detector" approach is almost 100% detection efficiency, as well being able to detect alphas and betas directly inside bulky large-mass target material. For example, leading double beta decay experiments have reached sensitivity of over 10^{26} y [1,2]. Within this approach, the alpha decay of ^{180}W with $^{116}CdWO_4$ [3] and ^{151}Eu with CaF_2(Eu) [4] crystal scintillators was registered at an experimental sensitivity level of over 10^{18} y. A recent and comprehensive review on rare decays

and techniques of their detection is given in [5]. However, the main disadvantage of the "source = detector" approach is the limitation to certain target elements which are suitable for detector manufacturing. Therefore, for many years, rare processes that could occur in elements such as Zr, Hf, Sn, Pt, Os, Pd, and Ru have not been explored at the highest sensitivity level due to the lack of scintillating material into which they can be embedded. Everything has changed after the first encouraging results on spectroscopic characteristics observed with Cs_2HfCl_6 (CHC) scintillating crystals in 2015 [6]. This crystal exhibits energy resolution of about 3% along with light yield comparable with that for NaI(Tl) standard scintillators. Consequently, this compound immediately attracted a significant attention from scientists from various fields.

Currently for high-sensitivity gamma-spectroscopy application there are needs for scintillators with targeted properties, such as a high light output (about 100,000 ph/MeV), excellent energy resolution (less than 3% at 662 keV line of ^{137}Cs), high stopping power (Z_{eff} larger than 70), fast scintillation decay time (less than 1 μs), good linearity down to low energies, and low cost. Thus, excellent scintillating performance in combination with the recent progress in Cs_2HfCl_6 crystals production opens up various applications, where such scintillators could be utilized along with commonly used high performance NaI(Tl), CsI(Tl), $LaCl_3$:Ce or $LaBr_3$:Ce scintillating crystals. However, further crystal production chain optimization aiming at general cost reduction should be addressed.

Despite that all above mentioned parameters are also required for Cs_2HfCl_6 crystals to be used in fundamental research, another characteristic of this material turns out to be even more attractive. Indeed, the unique feature of this material is the large fraction of the embedded Hf element of about 26% in mass. It should be stressed that these crystals are compounds with stable mechanical and optical properties over time, contrary to metal-loaded liquid scintillators that typically tend to the precipitation of heavy loaded scintillators and deterioration of their optical and spectroscopic properties. Hence, such a stable compound as a Cs_2HfCl_6 crystal with a high mass fraction of Hf, in combination with its high performance as a scintillating detector along with a relatively low internal background opens up new opportunities to search for rare nuclear processes occurring in Hf isotopes applying the "source = detector" experimental approach with an advanced sensitivity. As evidence that Cs_2HfCl_6 crystals are very promising in search for elusive nuclear processes, the rare alpha decay of ^{174}Hf isotope with a half-life of $T_{1/2} = 7 \times 10^{16}$ y was observed with only 7 g Cs_2HfCl_6 crystal acting as a scintillating detector (see Section 10 below, and [7]).

The Cs_2HfCl_6 compound crystallizes in a cubic structure with a lattice parameter $a = 10.42 \pm 0.01$ Å (space group Fm3m) that is isostructural to a potassium platinum chloride (K_2PtCl_6). Hence, the Cs_2HfCl_6 belongs into a group of compounds with a general formula of A_2MX_6, where A = Li, Na, K, Rb, Cs; M = Hf, Zr, Ti, Pt, Sn, Te; and X = Cl, Br, or I. Accordingly, each element in the Cs_2HfCl_6 crystal structure can be substituted for an alternative element with an equal ionic charge keeping the structural type unchanged. This makes the A_2MX_6 matrix very flexible to the element of interest that can be embedded. Therefore, controlled elements substitution would allow to use CHC-family crystals as scintillating detectors in experiments aiming to register rare processes (rare alpha, beta decay and neutrinoless double beta decay) that could occur in elements such as Zr, Sn, Pt, Os, Pd, and Ru, which have not been studied with the "source = detector" experimental approach at ultimate sensitivity.

While the first part of this review is dedicated to the analysis of progress in CHC-family crystals production, including the crystal growth, raw material purification, and conditioning procedures, the second part will cover aspects related to crystal characterization. This part would focus not only on preliminary light output estimation, scintillating decay components, and energy resolution evaluations, which are indeed very important and desired characteristics for gamma-spectroscopy, but it also will include consideration of material properties such as defect structure, quenching factor for alpha particles,

pulse shape discrimination ability, and internal radioactive background, which is of vital importance if the material is used in low-background experiments.

In view of the large number of articles related to this "hot" topic that have been published and may be under preparation, this review could be considered as the first attempt to systematize already existing results and achievements in CHC-family crystals growth, and to keep in one place the current status of these crystals studies, while providing hints for future investigations.

2. Cs_2HfCl_6 Crystal and Bromine-Containing Mixture Compounds

Despite the fact that Cs_2HfCl_6 compound was originally discovered as a luminescent material in 1984 by [8], it was re-invented as an attractive scintillator for gamma detection in 2015 by [6]. The best energy resolution that was measured with a ~1 cm^3 CHC crystal sample was calculated to be 3.3% at 662 keV under irradiation by ^{137}Cs gamma source (see Table 1), and this was obtained with a long shaping time of 12 μs. The light yield (with photomultiplier (PMT) readout) was estimated to be comparable to that of NaI(Tl) commercial crystal. The scintillation pulse was described with model that consists of two exponential components: fast decay time is 0.3 μs (5%) and slow component is 4.4 μs (95%). Authors also measured radioluminescence spectra and assigned the broad emission band that is centered at about 400 nm to an intrinsic luminescent center based on transitions of charge transfer type of the undisturbed $[HfCl_6]^{2-}$ anion complex, placed in the cubic hole created by Cs^+ ions at the corners of the cube.

Table 1. List of recently produced Cs_2HfCl_6 (CHC) crystals by different groups, crystal dimensions used for characterization (in case of cylindrical sample its diameter (∅) is also listed), the relative light yield (LY) and energy resolution (FWHM) measured under irradiation by 662 keV gamma line of ^{137}Cs source, and chemical purity of corresponding raw materials used for crystal growth. N.A. means "not analyzed".

Crystal Type	Dimensions or Volume, mm^3	LY, ph/MeV	FWHM, %	Chemical Purity, %		Ref.
				CsCl	$HfCl_4$	
Cs_2HfCl_6	650	54,000	3.3	99.998	99.9	[6]
	7 × 5 × 2	27,500	N.A.	99.999	99.5	[9]
	7 × 7 × 7	30,000	3.3	99.999	99.5 (2)	[10]
	∅22 × 20	36,000	4.0	99.9 (3)	99.9 (3)	[11]
	∅23 × 30	23,000	3.5	99.999	99.9 (4)	[12,13]
	∅10 × 15	23,000	2.8	99.999	99.9	[14]
	∅8 × 8	27,000	3.2	99.999	99.9 (4)	[14]
	∅25 × 8	N.D.	4.4	99.998	99.8 (1)	[15]

(1) Corresponds to additional 3-fold sublimation. (2) Corresponds to re-sublimation. (3) Corresponds to pre-synthesized CHC powder with a subsequent hydrochlorination. (4) Corresponds to additional 1-fold sublimation.

To grow this CHC crystal, the stoichiometric ratio of raw materials CsCl (99.998%) beads and $HfCl_4$ (99.9%, trace metals basis, excluding Zr) powder was properly mixed. No additional purification step was applied. All actions with the compound preparation were performed in a glove box under argon atmosphere, with moisture and oxygen levels maintained both below 1 ppm. It should be highlighted that in all below described experiments on CHC and CHC-family crystals growth, raw materials handling was performed in glove box with controlled atmosphere and reduced moisture, unless otherwise indicated. Vertical Bridgman furnaces were used for crystal growth. In this experiment, the CHC charge was melted at 820 °C and translated from a hot zone down to the cold zone at a pulling rate of (0.5–1.0) cm/day. The temperature gradient of 5 °C/cm was established at the solid/liquid interface. Crystals used for characterization were cut from the as-grown CHC boule. The CHC density was calculated to be (3.78 ± 0.04) g/cm^3, based on gravimetric measurements.

After this first demonstration of such promising scintillating characteristics of the CHC crystal, the comparative study of the luminescence and scintillation properties of Cs_2HfCl_6 and Cs_2ZrCl_6 crystals was performed by [9], where photoluminescence spectra, X-ray excited radioluminescence spectra, scintillation decay times, and pulse height spectra under irradiation with 662 keV gammas of ^{137}Cs source were analyzed.

CsCl (99.999%), $HfCl_4$ (99.5%), and $ZrCl_4$ (≥99.9%) powders were used as starting materials for synthesizing Cs_2HfCl_6 and Cs_2ZrCl_6 (CZC) crystals, accordingly. The powders were mixed in a stoichiometric ratio and dried by heating overnight at about 470 K in vacuum. Afterwards, the prepared mixtures were sealed in quartz ampules under vacuum, and then the vertical Bridgman method was used to fabricate crystals. The temperature gradient was set to 8.7 °C/cm, while pulling rate was at 1 mm/h. The CHC ($7 \times 5 \times 2$ mm^3) and CZC ($5 \times 4 \times 3$ mm^3) polished samples were used for crystal characterization and comparison. The X-ray fluorescence analysis revealed that the Cs_2HfCl_6 crystal contained Zr at a 0.12 mol% level. Meanwhile, the X-ray diffraction patterns of CHC and CZC samples indicated that both crystals contained a slight CsCl crystalline phase.

The X-ray-excited radioluminescence spectra of the CHC and CZC crystals measured at 300 K both have broad emission bands with main peaks at 398 nm wavelength for CHC, and 435 nm and 510 nm for CZC, correspondingly. Authors attributed the 398 nm emission of CHC crystal to the charge-transfer luminescence of the $[HfCl_6]^{2-}$ anion complex. The luminescence quantum yields of the Cs_2HfCl_6 and Cs_2ZrCl_6 crystals were estimated to be 55% and 29%, respectively.

Because scintillating pulses cannot be fitted with a single exponential model, authors have applied a double exponential assumption and fit averaged scintillating pulses with such model in the time interval up to 50 μs for CZC crystal and 200 μs for CHC crystal. The decay time constants were found to be about 2.2 and 8.4 μs for the Cs_2HfCl_6 crystal, and 1.5 and 7.5 μs for the Cs_2ZrCl_6 crystal, respectively. It should be emphasized that authors didn't introduce any deep physical meaning in the fitting model that contains two exponential functions, except a high quality fitting procedure. This point will be addressed later in the text (see Section 11). The scintillation light yield was estimated in comparison to the commercial NaI(Tl) crystal taking into account emission wavelengths of each crystal and spectral sensitivity of PMT at each peak wavelength. The scintillation light yields for Cs_2HfCl_6 and Cs_2ZrCl_6 crystals were estimated to be 27,500 and 25,100 photons/MeV, respectively.

In Ref. [10], Cs_2HfCl_6 (CHC) and $Cs_2HfCl_4Br_2$ (CHC4B2) crystals were grown from 99.5% $HfCl_4$ with 99.999% CsCl and 99.999% CsBr. Prior to synthesis, $HfCl_4$ powder was purified by sublimation at 300–400 °C. Then, starting materials were melted and compounded in stoichiometric ratio at 900 °C for at least 48 h to produce CHC and CHC4B2, correspondingly. Furthermore, synthesized CHC compound was sublimed after compounding prior subjecting to crystal growth, while CHC4B2 was not. This additional sublimation caused the difference in the final crystal boules. Along the perimeter of the CHC4B2 boule, numerous black inclusions were observed. A secondary phase accumulated primarily at the tail of the grown crystal and throughout its core, while the rest of the bulk was clear. On the contrary, CHC boules were clean inside being milky of the surface, and secondary phase precipitates in the core and boundaries of grains with the primary phase. The CsCl was identified by a micro X-ray fluorescence spectrometry to be this secondary phase, and its formation was explained as a result of a non-stoichiometric (CsCl-rich) melt composition. This could be due to an insufficient temperature or time required for the synthesis reaction, or due to the high vapor pressure of $HfCl_4$ during compounding. This secondary phase rich in CsCl was observed in CHC4B2 boule, as well.

Clean CHC sample had a light yield and energy resolution of 30,000 ph/MeV and 3.3%, respectively, and decay components of scintillating pulses of 0.39 and 3.9 μs (see Table 1). While, the sample of CHC4B2 crystal with a secondary phase present in the core had a light yield and energy resolution of 18,600 ph/MeV and 4.4%, correspondingly. The scintillating pulses show a faster decay with 0.38 and 2.0 μs components (see Table 2).

Table 2. List of recently produced $Cs_2HfCl_4Br_2$ and $Cs_2HfCl_4Br_3$ crystals by different groups, crystal dimensions (or volume) used for their characterization, the relative light yield (LY) and energy resolution (FWHM) measured under irradiation by 662 keV gamma line of ^{137}Cs source, and chemical purity of corresponding raw materials used for crystal growth. N.A. means "not analyzed".

Crystal Type	Dimensions or Volume, mm^3	LY, ph/MeV	FWHM, %	Chemical Purity, %			Ref.
				CsCl	CsBr	$HfCl_4/HfBr_4$	
$Cs_2HfCl_4Br_2$	∅10 × 13	18,600	4.4	99.999	99.999	99.5	[10]
	650	37,000	4.5	99.998	99.999	99.8 (1)	[16]
	∅23 × 26	20,000	3.7	99.999	99.995	99.9 (2)	[12,13]
	∅10 × 10	21,000	5.1	99.999	99.99	99.9	[14]
$Cs_2HfCl_3Br_3$	∅15 × 15	N.A.	N.A.	99.999	99.995	99.9 /98.5	[17]

(1) Corresponds to additional 3-fold sublimation. (2) Corresponds to additional 1-fold sublimation.

Authors also investigated one very important technological parameter of these crystals in light of their wide application—hygroscopicity and moisture sensitivity. Indeed, both crystals showed minimal moisture sensitivity. CHC developed a hazy surface between days 11 and 29, while CHC4B2 developed a hazy and then opaque surface layer after 30 and 48 h, respectively. Both samples showed minimal weight changes (<1 mg) within testing period.

Authors conclude that scintillating properties of CHC and CHC4B2 crystals make these materials appropriate for most low-counting rate applications. Moreover, an additional purification, alloying, or doping may also enhance scintillation performance. The investigation and development of alternate synthesis pathways (e.g., vapor-solid synthesis or wet synthesis) are needed to generate stoichiometric material for high quality crystal growth.

The complex work done by [11] should also be emphasized, wherein five different procedures of CHC crystal growth have been investigated in order to optimize growth conditions and scintillation properties. The authors proceeded from two approaches. The first approach was to develop a purer starting material that maintains stoichiometry better than just mixing binary halides. The second approach was to attempt to alter inclusion formation by adjusting crystal growth parameters, such as a thermal gradient, pulling rate, and crystal diameter.

Most of the CHC crystals obtained in this study were grown from the CHC charge produced following the procedure described below. An acid-saturated methanol solution was prepared by bubbling anhydrous HCl gas through 400 mL of ice-chilled methanol for 10 min. This acidic methanol solution was then diluted in a 1:10 ratio with fresh methanol to produce the reaction medium. Raw $HfCl_4$ powder (99.9% grade) was added in portions to the ice-cooled round bottom flask, followed by addition of CsCl grains (99.9% grade). The white precipitate of CHC compound was formed as the CsCl was added. This mixture was refluxed for 3 h under nitrogen and then stirred overnight at room temperature. Then, CHC powder was filtered out of the solution and washed twice with fresh methanol. The final CHC powder was then heated under vacuum at 120 °C in order to remove the remaining non-reacted methanol. The charge CHC powder, synthesized in above described way was loaded into a quartz ampule, dried at 100 °C for 12 h under vacuum and then sealed. Next, this material was overheated to 870 °C, while CHC melting point is about 810 °C, to separate secondary phases. After cooling, the obtained material was extracted and grounded. At the next step, the grounded charge material was loaded into an ampoule with two quartz frits to remove the high melting point secondary phases formed in the first step. The material was then melted through the filters for 24 h at 870 °C. This led to a complete separation of the secondary phases and all non-condition material and a single phase CHC, which was melted and passed through the frit. The filtered single phase CHC compound was then subjected to growth in the same ampoule. After the completion of growth, crystal boules were cooled to room temperature over 72 h.

Only one sample (crystal C) was grown from a CHC charge synthesized from raw CsCl and $HfCl_4$ powders in a stoichiometric ratio and then purified through hydrochlorinating. For this process, a portion of the pre-synthesized CHC compound was heated up to the melting point of 810 °C for 3.5 h under a flow of HCl gas.

Five crystals were grown in these studies and designated as crystals A to E. Crystal A (∅22 mm) was grown with a thermal gradient of 21 °C/cm and a pulling rate of 1 mm/h. Crystal B (∅22 mm) was grown with a higher thermal gradient of 34 °C/cm but the same pulling rate of 1 mm/h. Crystal C was grown in the same conditions as crystal B, except instead of using melt filtering to remove secondary phases, the material was hydrochlorinated. Crystal D (∅13 mm) was grown with a thermal gradient of 34 °C/cm and a pulling rate of 0.5 mm/h. While the crystal E (∅13 mm) was grown with a thermal gradient of 34 °C/cm and a higher pulling rate of 1 mm/h.

While X-Ray diffraction (XRD) measurements did not show difference in pattern for all analyzed crystals, the XRD spectrum of the black material shows the presence of hafnium oxide. Authors suggest that the hafnium oxide could be formed due to residual methanol or water from the synthesis reacting with the $HfCl_4$ at high temperature. As an indirect confirmation of this hypothesis could be the observation of black material presented at the top of the ampules is amorphous suggesting that it could be a carbon coating, created during the dissociation of methanol. The measurements taken with energy dispersive X-ray spectrometer (EDXS) were performed for each crystal on both the dark and the light regions, and demonstrate that the black regions are mainly composed of the CsCl phase.

Analyzing the set of CHC crystal samples obtained in growth runs with various gradient and pulling rate, variation of ampule diameter and other parameters authors noticed following effects: (1) an increase in thermal gradient resulted in less cloudiness or fewer inclusions in the bulk of the crystal; (2) a decrease in an ampule diameter results in a significant increase in the number of inclusions in the center of the crystal; (3) a decrease in the growth rate results in an effect similar to that of increasing the thermal gradient (the crystal sample is clearer near the core). As one possible explanation for the improvement in crystals quality that were grown at a higher thermal gradient or slower growth rate, authors suggest considering the constitutional supercooling.

In fact, the crystal sample C, that exhibits the best scintillating performance with an energy resolution (FWHM) of 4.0% at 662 keV gamma line and a light yield of (36,000 $\pm$ 500) ph/MeV (see Table 1), was grown in 22 mm diameter quartz ampule in thermal gradient 34 °C/cm and 0.5 mm/h pulling rate. Meanwhile, all obtained here CHC crystals exhibit superior proportionality with deviation from 1 less than 3% down to energy of 5 keV for gamma quanta, in comparison to SrI(Eu) scintillator with 6% or NaI(Tl) crystals with 15% deviation, respectively.

The radioluminescence emission spectra from the whole range of CHC crystals consist of a single peak with a maximum between 400 and 410 nm, and no other significant differences between spectra for crystals with different quality, beside just slight width variation of the emission peak. From this observation, the authors made the important conclusion that secondary phase of CsCl that could be present in CHC crystal is not producing a significant secondary emission.

The average scintillation pulses were fit with model contains two exponential components: 4.4 us (75%) and 1.0 us (25%). Meanwhile, for the purest crystal (hydrochlorinated material, sample C), these two components correspond to 5.8 us (86%) and 1.4 us (14%). This effect of scintillating kinetics elongation the authors attributed to its higher purity. Moreover, similarity of scintillating kinetics for CHC with different concentration of black inclusions within the crystals suggests that such inclusions are not affecting the mechanism of scintillation, while resulting in a stronger light scattering and absorption in the bulk. This hypothesis was confirmed by dedicated measurements of light absorption within CHC samples. The best performing CHC crystals offer the highest optical transmission in the region of 350–450 nm, which corresponded to the CHC peak emission, while crystals with the poorest performance exhibit the lowest transmission in that region.

To summarize, the authors suggested that the usage of the pre-synthesized CHC powder with a subsequent hydrochlorination and growth with a high thermal gradient maintains melt stoichiometry, and results in a nearly single phase CHC crystal with a high scintillating performance.

In 2019, the addition of bromine into the Cs_2HfCl_6 original lattice, resulting crystal structure and its scintillation properties were investigated in detail [16]. The main goal of that work was to provide improvements of CHC decay time of scintillating pulses, as the long decay time of 4.37 μs in initial compound limits the materials performance in a wide range of applications.

To produce $Cs_2HfCl_4Br_2$ starting materials were used 99.998% pure CsCl 99.999% pure CsBr, and 99.8% $HfCl_4$ powder (trace metals basis, exclusive of Zr). Before synthesis, the $HfCl_4$ powder was treated to three-fold static sublimation (with 50 g load each time) to reduce the concentration of low-vapor pressure contaminants. Each purification stage was performed at 400 °C for 12 h. After the third stage, the fraction of purified material was obtained nearly 80% of the initially loaded mass. The stoichiometric ratio of the purified starting materials was sealed in a quartz ampoule and maintained at 800 °C for 24 h to ensure the homogeneity of the CHC4B2 charge. The crystal was grown with a pulling rate of (0.5–1) cm/day and temperature gradient of 5 °C/cm at the solid/liquid interface. At the end of the crystal growth, the temperature of the furnace was uniformly cooled to room temperature in 72 h. Despite dedicated efforts and technological features, some precipitates were still observed in the central part of the crystalline boule.

Pulse height spectra were acquired with 10 μs shaping time under irradiation by ^{137}Cs gamma source, and demonstrated an energy resolution of 4.5% at 662 keV peak. The light yield was estimated to be 37,000 ph/MeV by comparison to a standard commercially available NaI(Tl) crystal (see Table 2). The light yield non-proportionality for CHC4B2 crystal was observed to be better (less than 1% deviation from 1) than for CHC crystal in the energy range of (20–400) keV. In addition to improved non-proportionality of scintillating response in CHC4B2, one would also expect better energy resolution than in CHC crystals due to a smaller band gap (3.7 eV), and consequently, larger number of photons at the same deposited energy. Moreover, the radioluminescence spectrum of CHC4B2 crystal, centered at 420 nm, makes it better spectrally matched with a SiPM device. Therefore, one could expect further energy resolution improvement with $Cs_2HfCl_4Br_2$ crystals coupled to such type of light detector.

The scintillation decay time response consists of two components: fast is 0.18 μs (8%) and a slow of 1.78 μs (92%), that is 2.5 times faster compared to previously reported for such type of crystal in [10]. This improvement of scintillation decay time authors attributed to reduction of CsCl secondary phase concentration, as well as to a quantum effect caused by the replacement of Cl^- ion with the heavier Br^- ions and breaking the symmetry the Hf_4^- activator ion. Shorter scintillation decay times are typically expected for heavier alkali halides. Authors are expecting to achieve further improvements of light yield and energy resolution through additional purification of raw materials.

Further progress in Cs_2HfCl_6 and $Cs_2HfCl_4Br_2$ crystals production was shown in [12]. As starting materials, CsCl (99.999%) and $HfCl_4$ (99.9%) for CHC, along with CsCl, CsBr (99.995%), and $HfBr_4$ (99.9%) for CHC4B2, were utilized. In this experiment, initial $HfCl_4$ powder of low chemical purity underwent an improved purification by a one-fold sublimation. There 200 g of $HfCl_4$ powder sealed in a quartz ampoule under high vacuum was placed into a single-zone horizontal furnace with temperature set to 220 °C. The sublimation process lasted for 72 h. For crystal growth stoichiometric amounts of corresponding starting materials loaded in quartz ampule and sealed under high vacuum were placed into a two-zone vertical furnace. The top furnace's zone temperature was set a few degrees above melting point of CHC or CHC4B2, while the bottom furnace's zone a few degrees below the corresponding melting point. The pulling rate was set at (3–4) mm/hour. The temperature gradient for CHC growth run was about 10 °C/cm, while for CHC4B2 was 12 °C/cm. When the growth cycle was completed both zones of furnace were cooled down

to room temperature at the rate of (100–150) °C/day. As described, transparent, clear, and crack-free 25 mm diameter Cs_2HfCl_6 and $Cs_2HfCl_4Br_2$ boules were obtained, and samples with dimensions of ∅23 × 30 mm^3 (CHC) and ∅23 × 26 mm^3 (CHC4B2) were cut for crystal characterization.

The response of CHC and CHC4B2 samples to gamma irradiation was measured by placing a crystal in a mineral oil within a quartz cup lined with Teflon tape as a diffuse reflector. The ^{137}Cs spectrum collected with a ∅23 × 30 mm^3 CHC sample showing an energy resolution of 3.5% (FWHM) at 662 keV, while the light yield was measured to be 23,000 ph/MeV (see Table 1). The light yield was evaluated by comparing the 662 keV full energy peak position for CHC with that of NaI:Tl taking into account the quantum efficiency of the PMT at 410 nm (emission peak of CHC) and at 415 nm (emission peak of NaI:Tl). The slightly lower light yield (LY) value for this sample, than previously reported in [10], authors attributed to not optimal light collection in those experimental conditions. The CHC4B2 sample demonstrates an energy resolution of 3.7% (FWHM) at 662 keV. The light yield, calculated with the same procedure as with CHC crystal, is 20,000 ph/MeV (see Table 2). It was suggested by the authors that better crystal quality contributes to a better energy resolution.

The averaged scintillating signals of CHC crystal were fitted with sum of two exponential functions, and decay time constants determined to be 0.25 μs (7%) and 3.8 μs (93%). In case of CHC4B2 crystal, the characteristic decay times were found to be 0.33 μs (10%) and 1.8 μs (90%). While the authors noticed that substituting some Cl^- ions with Br^- ions appears to halve the primary decay time from 3.8 μs to 1.8 μs, there are still no clear theoretical explanations of this phenomenon.

Next results of this group of researchers were published in [14], where the effect of raw materials purity on crystals scintillating properties was investigated. As starting materials were used CsCl (99.999%), CsBr (99.99%), and $HfCl_4$ (99.9%), respectively. To grow $Cs_2HfCl_4Br_2$ crystal, as-purchased raw materials in stoichiometric ratio were mixed. The first CHC crystal, CHC-1, was produced from a stoichiometric mixture of as-purchased raw materials with no additional purification. Meanwhile, the second CHC crystal, CHC-2, was produced from $HfCl_4$ powder that underwent an improved purification by a one-fold sublimation, as described in [12]. After materials loading, each ampoule was subjected to low temperature dehydration under high vacuum to remove moisture that might be introduced during loading and subsequent steps. Then, ampules were sealed and subsequently placed in a two-zone vertical furnace for crystals growth.

The response of CHC and CHC4B2 samples to gamma irradiation was measured with the same approach, as described in [12], where studied crystal was placed into a mineral oil. The ^{137}Cs energy spectrum collected with a ∅10 × 15 mm^3 CHC-1 sample, showing an energy resolution of 2.8% (FWHM) at 662 keV, and light yield was measured to be 23,000 ph/MeV. Energy resolution of 3.2% and light yield of about 27,000 ph/MeV were obtained for CHC-2 sample with slightly smaller dimensions, ∅8 × 8 mm^3 (see Table 1). The CHC4B2 crystal sample demonstrates an energy resolution of 5.1% (FWHM) at 662 keV and light yield of 21,000 ph/MeV (see Table 2, correspondingly). The light yield value for all studied crystals was evaluated by comparing the 662 keV full energy peak position for CHC/CHC4B2 with that of a commercial ∅25 × 25 mm^3 NaI:Tl crystal.

The averaged scintillating signals of CHC crystals were fitted with sum of two exponential functions, and decay time constants determined to be 0.25 μs (13%) and 3.3 μs (87%) for CHC-1, and 0.26 μs (12%) and 3.4 μs (88%) for the CHC-2 sample, correspondingly. In the case of CHC4B2 crystal, the characteristic decay times were found to be 0.19 μs (11%) and 2.9 μs (89%). Hence, one could notice that while for CHC crystals of different quality the kinematics of scintillation pulse is very stable, CHC4B2 crystals still demonstrate noticeable variation in the evaluated decay components for different crystal samples (see, for comparison, values reported in [12]).

The most recent progress in Cs_2HfCl_6 (CHC) and CHC-family crystals growth has been made at Fisk University was summarized in [13]. Since the vendors could only

provide Hf-halide compounds up to 99.9% purity level, impurities contained in these starting materials contributed much to inclusion and growth problems of the CHC and CHC-family compounds. Thus, a purification stage is required. The main difference in a purification process by an improved single-fold sublimation applied here to that as described in [12,14], was in a decrease of a loaded $HfCl_4$ or $HfBr_4$ powder for a single purification run, from 200 g to 150 g. Then, for each growth, a stoichiometric mixture starting materials were loaded into quartz growth ampoules that were pre-cleaned and baked at 700 °C. Loaded ampoules were attached at the dehydration-sealing station, where the mixed materials were then dehydrated at 90 °C for a few hours, and then sealed under high vacuum. Crystal growth was performed in a two-zone vertical furnace, following thermal conditions and pulling rates as described in [12] (see above).

At the beginning, 6.3% of energy resolution (FWHM) was measured for 7 × 7 × (4–5) mm^3 sample cut from the CHC crystal boule grown from unpurified raw materials. With samples retrieved from the CHC boule grown from purified precursors the improved energy resolution of (2.8–3.2)% at 662 keV was achieved. The results for samples from unpurified and purified by single-fold sublimation raw materials suggested that the purity level of the starting materials affected the CHC crystal quality and performance more than the influence of growth parameter alteration. Therefore, the next growth was performed with raw materials that were additionally purified, specifically sublimed-purified $HfCl_4$ (no details of this specific sublimation process listed in the cited article). The clear and transparent boule shows that both tuning growth parameters and employing purified starting materials improve the crystal quality.

At the last step, 25 mm diameter CHC crystal from additionally purified raw materials was grown, and the energy resolution of 3.5% (FWHM) at 662 keV was measured with a large ∅23 × 30 mm^3 CHC sample (see Figure 1 and Table 1), which is comparable to that earlier measured for crystals of smaller volume. A primary decay time between 3.5 and 4 μs is typical for CHC crystals and was obtained for both small and large volume crystals.

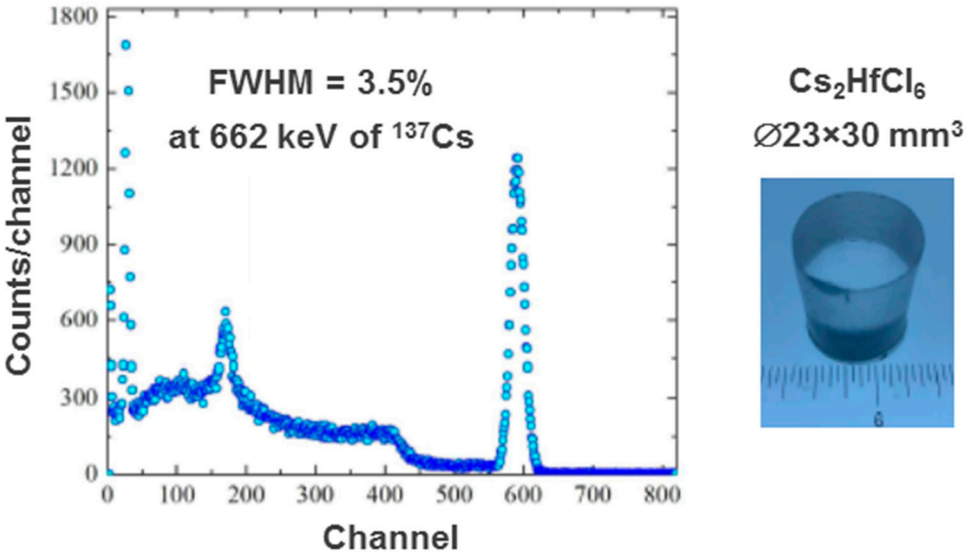

Figure 1. Pulse-height spectrum collected with a ∅23 × 30 mm^3 CHC crystal sample resulting in the energy resolution of 3.5% (FWHM) at 662 keV of ^{137}Cs gamma source (see [13] for more detail).

The same procedures, including the purification of starting materials, were followed also to grow CHC4B2 crystal. The energy resolution of 3.7% (FWHM) at 662 keV was measured for 25 mm diameter CHC4B2 crystal grown with purified starting materials (see Table 2). The primary decay time measured for this CHC4B2 sample is 1.8 μs.

Authors also perform the first studying of a permanent packaging of CHC crystals. An aluminum packaging with a quartz window was used as encapsulation. Prior to packaging, each sample was tested in a typical set-up with a mineral oil (see, for example [12]). The

energy resolution of 3.6% (FWHM) at 662 keV was measured with bare crystal, while after packaging this value slightly degrades to 3.9% (FWHM) at 662 keV.

Authors concluded that similar results, achieved both with small and large volume CHC crystals, indicate that crystal quality almost reached the highest level, and there is no internal scattering, absorbing centers, or impurities that reduce light output and prevent efficient light collection. Thus, the applied purification technique and growth conditions make it possible to produce large volume CHC crystals with the same performance as small size crystals.

While a number of articles are dedicated to $Cs_2HfCl_4Br_2$ crystal production and characterization, authors in [17] attempt to produce the $Cs_2HfCl_3Br_3$ (CHC3B3) crystal and investigate the effect of further constitution of Cl to Br ions. In order to synthesize $Cs_2HfCl_3Br_3$ compound the $HfCl_4$ (99.9%) and $HfBr_4$ (98.5%) powder, along with CsCl (99.999%) and CsBr (99.995%) beads were mixed in a stoichiometric ratio and sealed into a quartz ampule under vacuum. Then, the ampule was placed into a vertical furnace and pulled down with a speed of 1 mm/h during the crystal growth.

An obtained the CHC3B3 crystalline boule with rough dimensions $\varnothing 15 \times 15$ mm^3 had a yellowish color, contained many cracks and its surface was opaque, but the crystal was well transparent inside. Several crystal pieces were successfully fabricated from the obtained crystal boule for the optical measurements. Single crystal X-ray diffraction indicated that the CHC3B3 has a cubic Fm3m structure and the lattice constant was determined to be 10.67 Å. By substituting Br for Cl, the emission peak of CHC3B3 crystal was shifted when compared to CHC (415 nm) or $Cs_2HfCl_4Br_2$ (around 420 nm) towards longer wavelength region of 450 nm. The spectra of CHC3B3 also had a broad shoulder around 530 nm. The scintillation decay was fitted by a single exponential function and decay constant was estimated to be (2.2 ± 0.3) μs. Such results might suggest that halogen substitution causes the emission wavelength shift for CHC with increasing the atomic number of substituted halogen atoms, i.e., Br and I, while the scintillation decay slowed down with high content of Br in the Cl sub-lattice, in comparison to CHC4B2 crystal with decay time of about 1.8 μs. No estimation on relative light yield was made with those samples (see Table 2).

The synthesis of a single-phase stoichiometric Cs_2HfCl_6 material, as could be seen from above discussed researches, is an uneasy task due to the $HfCl_4$ high volatility and hygroscopicity, and kinetics of the CsCl and $HfCl_4$ reaction in solid phase. CHC crystal growth suffers from CsCl-phase precipitation, which leads to inclusions in the first-to-freeze sections, compound decomposition, and non-stoichiometry. Thus, the successful growth of high-quality CHC crystal requires complete synthesis of this compound and removal of oxygen-containing impurities before growth process. Therefore, besides an extensive characterization of scintillating properties of CHC crystal, it is vital to characterize the behavior of Cs_2HfCl_6 as a chemical compound under different thermal treatments. The former will help to improve the technological procedure and thermal regimes of Cs_2HfCl_6 charge synthesis and crystal growth.

Authors in [18] prepared a high-quality single-phase undoped Cs_2HfCl_6 crystal and described material stability and thermal behavior by the simultaneous non-isothermal differential scanning calorimetry and thermogravimetry (DSC–TG) analysis. In addition, the influence of various atmospheres (nitrogen and vacuum) and conditions (enclosed system in a sealed quartz ampule) on the CHC compound stability were investigated. This study contributes to the improvement and optimization of the thermal conditions for CHC crystal growth from the melt by the Bridgman method. First, the congruent melting point was determined to occur at ca. (821–822) °C. The temperature position of the effect was the same even at 10-cycle measurement, pointing to the reversibility of the observed effect and its stability. Similarly, no undercooling of Cs_2HfCl_6 compound was determined as the solidification occurred at practically similar temperature of ca. (822–824) °C. This indicates that the Cs_2HfCl_6 solidification occurs at a similar temperature as its melting. Such a result is not common in halides as high undercooling was observed, e.g., in $PbCl_2$ [19] and $CsCaI_3$ [20].

In this study, it was also shown that the CHC compound decomposition occurred at 300 °C under vacuum, while under N_2 atmosphere CHC stay without significant mass losses until the eutectics at 587 °C. Such high temperature instability could limit the Cs_2HfCl_6 crystal application as a scintillator since CHC crystal luminescence and scintillating properties are strongly correlated with its chemical composition and stoichiometry.

It is necessary to mention research reported in [21], where the question of doping of CHC crystal by Te^{4+} ions was addressed. In this study the photoluminescence (PL) and scintillation properties of 1.0, 3.0, 5.0, and 10 mol% Te^{4+}-doped Cs_2HfCl_6 crystals were investigated along with photoacoustic (PA) spectroscopy, which enables direct monitoring of the non-radiative de-excitation processes that take place in the sample after absorption of irradiation energy. There, Cs_2HfCl_6 crystal plays the role of host material, since the $(HfCl_6)^{2-}$ octahedra have a perfect octahedral symmetry and do not share anions, i.e., the tetravalent metal ions, such as Zr^{4+}, Te^{4+}, Sn^{4+} Pt^{4+}, Os^{4+}, etc., can occupy the center of an undistorted $(HfCl_6)^{2-}$ octahedron. For this reason, CHC-family crystals appeared to be ideal as model compounds for investigating the photoluminescence properties of tetravalent metal ions.

In this study unusual cleaning procedure was applied to quartz ampules. Quartz ampoules were cleaned in a strong alkali solution to remove organic impurities and then were thoroughly rinsed with ultrapure water. As a second step, ampoules were annealed at 1000 °C for 24 h. Afterwards, the stoichiometric mixture of CsCl (99.99%), $HfCl_4$ (99.9%), and $TeCl_4$ (99.9%) raw materials without any additional purification were loaded into the clean ampoules, dried under vacuum at 300 °C for 24 h, and then sealed. Crystals were grown in two-zone vertical furnace at the temperature gradient of 13 °C/cm and at the pulling rate of (24−48) mm/d. Crystal samples for whole range of doping concentrations have a yellowish color and visible cracks induced during the crystal growth and cooling processes. Samples with dimensions 2.0 × 2.0 × 1.0 mm^3 were sliced and polished to be used in further measurements.

The radioluminescence spectra exhibited a yellow emission band peaking at 575 nm. The scintillation intensity for the 3.0 mol% Te^{4+}-doped crystal was the highest among studied crystals. The decay time of scintillation pulses is in agreement with a three-exponential function, with primary, secondary, and tertiary decay time values of 0.02 μs (2%), 0.63 μs (18%), and 2.34 μs (80%), respectively. The value of the dominant two decay components is consistent with that of the corresponding PL values, which are due to transitions of Te^{4+} ions. The origin of the primary fast component was not clearly understood, but it could be due to the quenching of the intrinsic emission of the CHC host with an efficient energy transfer to Te^{4+} ions. Scintillating pulse decay components decreased with increasing of Te^{4+} dopant concentration.

The pulse height spectra under irradiation by ^{137}Cs gamma source were recorded with a 6 μs shaping time. The scintillation light yield of the samples was calculated by comparing the determined 662 keV gamma line photopeak position in the spectrum with that of a CsI:Tl (LY = 54,000 ph/MeV, wavelength of the emission maximum (λ_{em}) = 550 nm) under the same experimental conditions. The scintillation light yield of the Te^{4+}-doped crystals was estimated to be approximately 11,700 (Te, 1.0 mol%), 13,100 (Te, 3.0 mol%), 9600 (Te, 5.0 mol%), and 9000 (Te, 10 mol%) ph/MeV. Energy resolution was not quoted for these measurements (see Table 3).

The measurement of photoacoustic (PA) spectrum was performed with a custom setup, where a xenon-lamp was used as the excitation source and a monochromator combined with a mechanical chopper plays the role of the optical system. The excitation light was modulated by the mechanical chopper at 20 Hz frequency. The acoustic signal was detected with the sample being placed in a customized PA cell fitted with an electret microphone. The output signal from the microphone was amplified by a preamplifier and then fed into a lock-in-amplifier with a reference signal input from the chopper. Finally, the signal from the lock-in-amplifier was converted into a digital form and transmitted for analysis by computer through a digital multi-meter. The spectra were normalized for changes in the

excitation light intensity using carbon-black as reference. As a result, an inverse correlation between scintillation light yield and PA intensity with different Te-concentrations was confirmed experimentally. This study is interesting in the field of scintillating materials investigation, where the main focus will be on studying the energy transfer mechanism between $(HfCl_6)^{2-}$ complex ion and dopant ions using thermal measurements of the photoluminescence spectrum and decay curves.

Table 3. List of Cs_2HfI_6 crystals doped by Te in with different concentrations, Tl and Ce ions, crystal dimensions (or volume) used for their characterization, the relative light yield (LY) and energy resolution (FWHM) measured under irradiation by 662 keV gamma line of ^{137}Cs source, and chemical purity of corresponding raw materials used for the crystal growth. N.A. means "not analyzed".

Crystal Type	Dimensions or Volume, mm^3	LY, ph/MeV	FWHM, %	Chemical Purity, %			Ref.
				CsCl	$HfCl_4$	$TeCl_4$	
CHC:Te 1 mol%	2 × 2 × 1	11,700	N.A.	99.99	99.9	99.9	[21]
CHC:Te 3 mol%	2 × 2 × 1	13,100	N.A.	99.99	99.9	99.9	
CHC:Te 5 mol%	2 × 2 × 1	9600	N.A.	99.99	99.9	99.9	
CHC:Te 10 mol%	2 × 2 × 1	9000	N.A.	99.99	99.9	99.9	
CHC:Tl 0.08 mol%	3.5 × 2.5 × 1	23,700	N.A.	99.999	99.9	99.9 (1)	[22]
CHC:Ce 0.15 mol%	5 × 3 × 1	15,700	N.A.	99.999	99.9	99.9 (2)	

(1) Corresponds to 99.9% grade of TlCl powder. (2) Corresponds to 99.9% grade of $CeCl_3 \times 17H_2O$ powder.

Another attempt to grow doped CHC crystals was described in [22]. In this study, the luminescence and scintillation properties of Tl- and Ce-doped CHC crystals was investigated. Stock powders of CsCl (99.999%), $HfCl_4$ (99.9%), TlCl (99.9%), and $CeCl_3 \times 17H_2O$ (99.9%) compounds were used for the synthesis of corresponding charges. The mixtures in stoichiometric ratio were dried by heating over 150 °C for 12 h under vacuum. Then, mixtures were sealed in quartz ampules and crystals were grown at a temperature gradient of 8.7 °C/cm and a pulling rate of 1.0 mm/h in the vertical furnace. As-grown CHC:Tl and CHC:Ce boules were cut and polished to sizes of 3.5 × 2.5 × 1 and 5 × 3 × 1 mm^3, respectively.

It should be noted that actual Tl and Ce concentrations measured by mass-spectrometry technique in the grown crystals, 0.08 mol% and 0.15 mol%, were significantly lower than those in the corresponding melt, 0.5 mol% and 0.2 mol%, respectively. However, no clear idea has been proposed to explain such unexpectedly low Tl-concentration in the final crystal, the lower Ce-concentration was explained by differences in the ionic radii and charges of the impurity (Ce^{3+}) and host (Cs^+) ions.

RL bands for Tl- and Ce-doped CHC crystals were observed at 405 and 430 nm, respectively. The 405 nm band can be attributed to the same origin as undoped CHC. While the 430 nm band authors attributed to charge-transfer transitions in $[HfCl_6]^{2-}$ or complex ion luminescence from $[ZrCl_6]^{2-}$ impurities, no extrinsic luminescence originating from the dopants in either the Tl- or Ce-doped CHC crystals was observed by RL spectroscopy. The authors explained this by a low concentration of dopant ions.

Scintillation decay time constants were obtained using the double exponential assumption. Decay time constants were found to be about 0.6 μs (24%) and 4.1 μs (76%) for CHC:Tl crystal, and 1.2 μs (33%) and 6.1 μs (67%) for CHC:Ce sample. The light yield was estimated in comparison to that of Gd_2SiO_5:Ce (GSO:Ce), using the photopeak position of 662 keV gammas. Assuming that the light yield of GSO:Ce crystal is about

10,000 ph/MeV, the light yield for CHC:Tl and CHC:Ce crystals was estimated to be 23,700 and 15,700 ph/MeV, respectively (see Table 3). The authors explain the lower light yield for doped crystals compared to undoped CHC, by the low energy transport efficiency from the host to dopant ions.

3. Iodine-Containing Substituted Compounds

Scintillation materials with a high light output, high effective atomic number (Z_{eff}), and low intrinsic radioactive background are required for a high sensitivity gamma-ray spectrometry. This is generally because the light output increases with the band-gap (E_{gap}) of the host material decreasing, crystals with a small-E_{gap} are expected to have higher light output. Therefore, in order to improve the light output of CHC crystals (about of 30,000 ph/MeV), some groups are focused on the effect of anion substitution resulting in a valuable E_{gap} decrease.

Following this idea, one group of researchers performed anion-substitution for Cs_2HfCl_6 (CHC) scintillator, and then succeeded to grow Cs_2HfI_6 (CHI) single crystalline scintillator with high light output of about 70,000 ph/MeV at 700 nm peak emission, as was mentioned in [22]. By complete substituting I^- for Cl^-, i.e., obtaining Cs_2HfI_6 (CHI), band-gap of CHC (E_{gap} = 6.4 eV) decreases to 3.9 eV. However, its scintillation decay time of 2.5 μs remains still rather slow for a practical use as a gamma-ray detector, since shorter decay time (less than 1 μs) is required. In their later study [23], authors performed Ce^{3+}/Eu^{2+} doping to improve decay time of CHI, introducing the fast 5d-4f luminescence.

In this study, Ce and Eu doped CHI compounds were synthesized from CsI (99.999%), HfI_4 (99%), CeI_3 (99.9%) and EuI_2 (99.99%) as starting materials. Each mixed powder with nominal composition of Cs_2HfI_6 with 1 at% of Ce^{3+} or Eu^{2+} admixture was inserted into a quartz ampoule and baked at 120 °C for over 6 h to remove moisture, and only then sealed under vacuum. Each ampoule was set into a vertical furnace and heated by radio-frequency induction to 750 °C (the melting point of undoped CHI), and after visual confirmation of charge melts, the ampoule was pulled down at 0.18 cm/h, and then it was gradually cooled down to room temperature. Authors succeeded in growing CHI:Ce and CHI:Eu and undoped CHI reference crystals. All crystals had orange/red color and extremely low transparency. Crystal boules were 0.8 cm in diameter and about 2.5 cm long. The space group Fm3m was confirmed for doped CHI:Ce and CHI:Eu crystals by X-ray diffraction measurements. The combination of X-ray diffraction and ICP-OES measurements leads to conclusion that (0.3–0.5)% of Hf site could be substituted by Zr ion impurity. Lattice constants of both of CHI:Ce and CHI:Eu crystals were calculated to be 11.61 Å. From the results of ICP-OES measurements a slight segregation of Cs element in CHI:Ce and CHI:Eu crystals was observed, and roughly estimated the effective segregation coefficients of Ce and Eu as <1 and ≈1, respectively.

Light output of CHI:Ce was estimated to be about 48,000 ph/MeV (see Table 4). As for CHI:Eu, the light output was about 69,000 ph/MeV. The energy resolutions of CHI:Ce and CHI:Eu were estimated to be 12.0% and 8.0% at 662 keV gamma line of ^{137}Cs using the PMT, respectively. High values of light output measured for all studied crystals could be explained because of small band gap in the CHI compound. Therefore, even a very low transparency of crystal samples cannot hide this effect.

The scintillation decay curves of CHI:Ce and CHI:Eu samples were fitted using a single-exponential component in time interval up to 18 μs. CHI:Ce and CHI:Eu crystals had characteristic decay times of 2.3 μs and 2.8 μs, respectively. Authors concluded that the effect of Ce/Eu doping on the radioluminescence spectra is negligible, since CHI:Ce, CHI:Eu and undoped CHI all show a broad emission in the red-orange region around (500–800) nm with a maximum at 700 nm. Although the luminescence intensity partially changed, 5d-4f or 4f-4f electron-transition luminescence of Ce^{3+}/Eu^{2+} was not observed. Therefore, authors assumed that the intensity change for the Ce/Eu doped CHI crystals can be ascribed to the crystal lattice defects.

Table 4. List of Cs_2HfI_6 crystals produced by different groups, crystal dimensions (or volume) used for characterization, the relative light yield (LY) and energy resolution (FWHM) measured under irradiation by 662 keV gamma line of ^{137}Cs source, and chemical purity of corresponding raw materials used for crystal growth.

Crystal Type	Dimensions or Volume, mm^3	LY, ph/MeV	FWHM, %	Chemical Purity, %		Ref.
				CsI	HfI_4	
Cs_2HfI_6	few	70,000	10.4	99.999	99	[23]
Cs_2HfI_6:Ce	few	48,000	12.0	99.999	99	[23]
Cs_2HfI_6:Eu	few	69,000	8.0	99.999	99	[23]
Cs_2HfI_6	$3 \times 4 \times 1$	64,000	4.2	99.999	99	[24]

Although the first scintillating performance of CHI crystal was promising, crystal growth conditions had not been optimized yet. It was remarkable with energy resolution that was estimated with a Si avalanche photo-diode (Si-APD) to be of about 10.4%, which is much worse than expected, because of the light scattering inside the crystal. Thus, authors made a further step in the CHI crystal production technology improvement.

As reported in [24], the CHI compound was synthesized from CsI (99.999%) and HfI_4 (99%) powders as raw materials, which were mixed in stoichiometric ratio and sealed under vacuum. The ampoule was heated up to melting point of CHI in vertical furnace and then pulled down from the hot zone to the cool part with a speed of 0.06 cm/h, about 3 times slower than in previously reported pulling rate (0.18 cm/h). Since the obtained CHI crystal boule consisted of a transparent part with no cracks, it was possible to prepare one transparent single crystalline specimen with dimensions of $3 \times 4 \times 1$ mm^3.

With this sample remarkable improvement of scintillation performance was achieved, especially in energy resolution, and it was caused by reducing the CHI crystal growth speed. The scintillation light output and energy resolution measured with a Si-APD were evaluated to be about 64,000 ph/MeV and 4.2% at 662 keV, respectively (see Table 4). The scintillation decay curve was acquired with a PMT, fitted with a single-exponential model and measured to be 1.9 μs. Authors noticed that by slowing growth speed, the inclusions of bubbles or pores seem to be suppressed, which leads to an improvement in energy resolution caused by the suppression of scattering and self-absorption of scintillation light inside the CHI crystal due to improvement of its transparency. It should also be highlighted that CHI crystal obtained in this study had the highest light output and the best energy resolution among red-orange emitting scintillators.

4. Tl-Containing Crystals

Significant and impressive progress in CHC crystals growth technology improvement and its high scintillating performance triggered further studies of compounds from the same family, but which would better satisfy requirements for scintillating materials in gamma-spectroscopy in terms of a high stopping power, i.e., high Z_{eff}.

In 2018, two independent groups of authors, reported about success in Tl_2HfCl_6 (THC) and Tl_2ZrCl_6 (TZC) crystals growth and very encouraging results after first testing of its scintillating characteristics. First group [25] came to these compounds as a result of sequence studies of crystals such as Rb_2HfCl_6 and Cs_2HfBr_6 that demonstrated high scintillating light yield and good energy resolution without any dopant. Following this route and trying to further profit from high Z of Tl-ions, authors focused on Tl_2HfCl_6 and Tl_2ZrCl_6 crystals, which having high Z_{eff} results in excellent photoelectric conversion efficiency for X-rays and gamma quanta. Crystals were grown from raw materials of commercial grade (TlCl—99.9%, $HfCl_4$—99.9%, and $ZrCl_4$—99.99%) without any additional purification step. Small samples with dimensions about $2 \times 1 \times 1$ mm^3 were used for crystal characterization. Both crystals showed broad radioluminescence spectra with emission band peak at 450–470 nm. Scintillating signals were fitted by sum of two exponential decay components with characteristic times of 0.29 μs and 6.34 μs for THC, and 0.70 μs and 2.36 μs for TZC

crystal. Scintillating light yield was estimated in comparison to commercial NaI(Tl) crystal. It was approximately estimated to be 24,200 and 50,800 ph/MeV for THC and TZC crystals, respectively. Energy resolution acquired at the 662 keV gamma line was 17.7% for THC and 5.6% for TZC, correspondingly (see Table 5 below).

The second group [26], initially focused only on the production of TZC crystals. Commercial raw materials TlCl (99.999%) and $ZrCl_4$ (99.9%) without any purification step mixed in stoichiometric ratio were used for synthesis of the TZC compound. A transparent crack-free sample with dimensions 8 × 8 × 1.5 mm^3 was used for crystal characterization. A broad band in radioluminescence spectrum in the range 350–700 nm with a peak at 468 nm was observed. The luminescence in TZC crystal was assigned to the charge transfer in the $[ZrCl_6]^{2-}$ anion complex or self-trapped exiton (STE) emission. From the pulse height spectrum acquired under irradiation by ^{137}Cs gamma source, 4.3% of energy resolution was achieved. The light yield was estimated to be (47,000 ± 4,700) ph/MeV, comparing to $Lu_{1.8}Y_{0.2}SiO_5$:Ce (LYSO) crystal (see Table 5). This high value of the measured light yield was explained by authors reminding that Tl^+ ion has a higher electronegativity than the alkali ion [27], thus band gap could decrease, which leads to increase of LY for the same energy deposition.

Table 5. List of recently produced Tl_2HfCl_6 and Tl_2ZrCl_6 crystals by different groups, crystal dimensions (or volume) used for their characterization, the relative light yield (LY) and energy resolution (FWHM) measured under irradiation by 662 keV gamma line of ^{137}Cs source, and chemical purity of corresponding raw materials used for crystal growth.

Crystal Type	Dimensions or Volume, mm^3	LY, ph/MeV	FWHM, %	Chemical Purity, %			Ref.
				TlCl	$HfCl_4$	$ZrCl_4$	
Tl_2HfCl_6	2 × 1 × 1	24,200	17.7	99.9	99.9		[25]
	∅7 × 5	32,000	4.0	99.999	99.9 (1)		[28]
	∅10 × 5	18,000	9.0	99.99	98		[29]
	∅16 × 16	27,000	3.7	99.99	99.9 (1)		[13,30]
	≈10	20,000	5.0	99.99	99.9 (2)		[31]
Tl_2ZrCl_6	2 × 1 × 1	50,800	5.6	99.9		99.99	[25]
	8 × 8 × 1.5	47,000	4.3	99.999		99.9	[26,32]
	∅10 × 5	40,000	5.4	99.99		99.9	[29]
	∅16 × 16	35,000	3.4	99.99		99.9(1)	[13,30]

(1) Corresponds to additional sublimation. (2) Corresponds to crystal grown from flux.

A bit later, results on the excellent pulse shape discrimination (PSD) achieved with the same TZC crystal sample (8 × 8 × 1.5 mm^3) under irradiation by 662 keV gamma quanta of ^{137}Cs and 5.48 MeV external alpha particles from ^{241}Am sources were published in [32]. The energy resolution was calculated to be 4.3% for 662 keV gammas (see Table 5) and 6.5% for 5.48 MeV alphas, correspondingly. Slightly worsened energy resolution for alpha particles was explained by roughness of the crystal surface and possible light leakage through the hole for alpha particle irradiation in Teflon tape wrapping crystal. The quenching factor (QF) was estimated to be 0.29. By more careful fitting of the scintillating pulses with a model that contains three exponential components, authors achieved excellent particle discrimination. For example, with optimum filter method the factor of merit (FOM) parameter was calculated to be 3.5, and it is higher than for CLYC crystal (FOM > 3). The greater FOM value indicates that alpha particles can be clearly separated from gammas in the energy range from 500 to 2000 keVee.

The best energy resolution of 4.0% FWHM at 662 keV was obtained with a 5 mm thick THC sample in [28]. This significant improvement in the energy resolution in comparison to earlier published values (17.7%) was assigned to a better crystal quality due to the modified method of growth. As well as the separation of impurities by the sublimation resulted in a better quality crystal, leading to a notable improvement in the scintillation characteristics. The light yield of the THC crystal was estimated by comparing its 662 keV photopeak position with that of a calibrated LYSO:Ce scintillating crystal, and it was calculated to be

(32,000 ± 3,200) ph/MeV (see Table 5). Scintillating pulses under gamma quanta excitation consisted of three decay constants 0.36 μs, 1.04 μs and 14.9 μs with relative amplitudes 18.9%, 61.2% and 19.8%, respectively. At the same time, pulses under irradiation by alpha particles were described by fitting with four components—0.09 μs (8.5%), 0.46 μs (28.9%), 1.04 μs (44.9%) and 11.2 μs (18%). The quenching factor was estimated to be 0.34 for 5.4 MeV alpha particles. This crystal also exhibited a great pulse shape discrimination ability for alpha particle and gamma quanta with FOM of 2.6.

It should be noticed that detection efficiency of the THC crystal to a full absorption peak was significantly higher in comparison to CHC due to the presence of heavy Tl^+ ions. For example, the detection efficiency of 3 cm thick THC crystal at the energy of 3 MeV was 280%, 220%, and 170% better than those for the NaI(Tl), CHC and $LaBr_3$ crystals, respectively.

Moreover, very recently, the PSD ability was demonstrated for TZC crystals not only for gamma quanta and alpha particles, but also for neutrons and protons [29]. Owing the presence of ^{35}Cl in its chemical formula (Tl_2ZrCl_6), fast neutrons can be detected though (n,p) and (n,alpha) nuclear reactions. Three different clusters of signals were detected under irradiation of the TZC crystal by AmBe source, and ascribed to registration of gammas, alpha particles, and protons. Thus, this material is a potential candidate for both high energy neutrons and gamma detection and spectroscopy.

A group of authors [31] implemented one alternative way to grow THC from raw materials with purity grade TlCl (99.99%) and $ZrCl_4$ (99.9%), using a low melting point halide flux (with melting point less than 350 °C) to control a high vapor pressure of $HfCl_4$ component. They succeeded in obtaining the THC crystal sample with volume of about 1 cm^3 and to characterize it. The light yield of this THC crystal was estimated in comparison to $Bi_4Ge_3O_{12}$ (BGO) scintillating crystal, and calculated to be about 20,000 ph/MeV. The energy resolution at that energy was about 5% (see Table 5).

To date, the largest volume of high-quality THC and TZC crystals was grown by group [30]. This group is well-known because of the re-invention of CHC crystal in 2015 [6]. Since then, all efforts have been focused into production of large volume high-quality CHC-family crystals with a highest scintillating performance. In this study, the THC and TZC crystal boules were grown from raw materials with purity grade TlCl (99.99%), $HfCl_4$ (99.9%) and $ZrCl_4$ (99.9%), and following purification and growth procedures as described in [13] for production of the high quality CHC crystal. At the end, transparent and crack-free crystal boules with outer diameter of 16 mm and about 80 mm long were obtained. For crystal characterization, samples with ∅16 × 16 mm^3 rough dimensions were cut by diamond saw and polished up to 4000 grit Al_2O_3 polishing pad. This group typically utilizes unusual method to measure scintillating light yield and energy resolution of crystals under gamma source irradiation. Here, crystal samples were placed into a quartz cup filled with a mineral oil and wrapped by Teflon tape on lateral side, while top was closed by Teflon sheet. In that configuration, one could expect to achieve light output enhancing due to minimization of refraction index mismatch between THC/TZC crystals and mineral oil, and later, this extracted scintillation light is more effectively redirected to the PMT window by diffuse reflector (Teflon tape and sheet) with further homogenization. Both these parameters lead to an improvement of the relative light yield and energy resolution detected with a crystal in such configuration.

The energy resolution of 3.7% was measured for the THC crystal sample under irradiation by 662 keV line of ^{137}Cs gamma source, while energy resolution of 3.4% was achieved with the TZC crystal. It should be noticed that these values of energy resolution are the best among all quoted up to date for those scintillating materials. The relative light yield of 27,000 ph/MeV for THC and 35,000 ph/MeV for TZC was measured, respectively (see Table 5). Primary decay times improve from about 4 μs for CHC to about 1 μs for THC and 2 μs for TZC, which makes these compounds more preferable in gamma-spectroscopy applications.

Brief information about recently produced THC and TZC crystals by different groups are listed in Table 5, including the chemical purity of used raw materials and additional conditions (like a low temperature flux or additional sublimation of raw materials), dimensions of crystal samples used for its characterization, relative light yield, and energy resolution measured under irradiation by 662 keV gamma line.

All authors noticed that further improvements of the light yield and energy resolution may be pursued through additional purification of raw materials and crystal growth process modification. An obvious path is the further purification of Hf and Zr-halides, since market available purity grade is no more than 99.9%, which is less than required for a high-quality crystal production. One should aim for chemical purity of about 99.999%, and only in that case the highest quality crystals are expected to be produced in furnaces with optimized thermal gradient and growth conditions. For example, previously produced CHC crystals from additionally purified $HfCl_4$ powder by multi-fold sublimation exhibit better scintillating properties than one produced from as-received raw materials, as was described above in CHC section.

THC and TZC crystals, where Cs^+ ions are substituted by Tl^+ ions, possessed higher density, effective atomic number (Z_{eff}) and faster scintillation kinetics, and all these parameters are vital for enhancing an X-ray/gamma-ray detection efficiency. Therefore, recent measurements and characterization mostly focused on its preliminary light yield evaluation, energy resolution determination and scintillating pulses decay times estimation. From achieved results, it is clear that these materials are very promising for homeland security, nuclear proliferation, gamma spectroscopy and other applications, like fast neutrons detection via reactions on ^{35}Cl isotope. For the moment, there are no results of measurements aiming to evaluate its internal radioactive contamination (internal background) that will help to understand applicability of such crystals in fundamental research looking for rare nuclear processes or other low-background applications. Typically, scintillating materials should contain radioactive nuclides on the activity level of about 1 mBq/kg, or less. Such a demanding radiopurity level can only be achieved by careful selection of raw materials from suppliers that provide the lowest initially radioactive contamination, as well as through the use of highly effective purification and synthesis technologies.

5. Pulse Shape Discrimination

The investigation of the pulse shape discrimination (PSD) ability with the Cs_2HfCl_6 crystal was performed for the first time in [15]. The pulse shape of scintillation light events in the CHC crystal 25 mm in diameter and 8 mm in height were studied under irradiation by alpha particles from an external ^{241}Am source and gamma quanta from ^{137}Cs gamma source. The crystal was irradiated through the top-face, opposite to the side coupled to the PMT, for five minutes with gamma and alpha sources independently. About 5000 events of each type were collected for the central part of corresponding peaks, so-called "pure" events, and used for further off-line analysis. Scintillating signals were acquired and recorded for the time interval up to 25 μs. Then the average of 5000 "pure" gamma and alpha waveforms were fitted within the entire time interval with the sum of four exponentials. Decay constants and their corresponding amplitudes for gamma events were determined as following 5.34 μs (81.2%), 2.11 μs (14.8%), 0.56 μs (3.3%), and 0.15 μs (0.7%). While for alpha events these four pulse components were defined to be 5.04 μs (74.2%), 1.64 μs (18.5%), 0.44 μs (5.9%), and 0.11 μs (1.4%).

This substantial re-distribution of the excitation energy from interaction event between scintillating pulse components allows one to distinguish between gamma and alpha events with the pulse shape discrimination technique. Indeed, in study [15], three different methods were used, namely optimum filter, mean time, and charge integration analysis (fast/total ratio), and all three show excellent discrimination between events initiated by particles of different type. By the optimum filter and the mean time methods, a factor of merit (FOM) of 9.3 and 7 were achieved, respectively. The charge integration technique provides the separation between peaks with a FOM of 7.5. All these results display that

signals originating from alpha and gamma irradiation can be clearly distinguished from each other in CHC crystals. This study was an essential step in the development of a highly sensitive low-background Hf-containing detector aiming to search for rare alpha decays occurring in natural Hf isotopes. The efficiency of pulse shape discrimination with CHC crystal one can see in Figure 2, where a mean time versus energy scatter plot for the data collected in low-background measurements with the 7 g CHC scintillating crystal over 2848 h [7] is presented. One can see a clear separation of events distribution originated by alphas and betas/gammas.

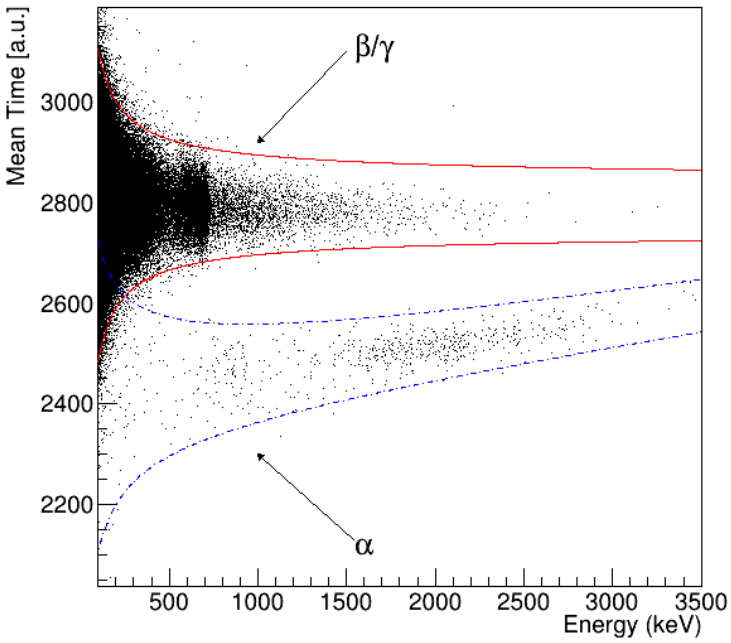

Figure 2. Mean time versus Energy scatter plot for the data collected in low-background measurements with the 7 g CHC scintillating crystal over 2848 h [7]. The mean time values corresponding to for alphas or betas/gammas events, along with intervals containing 99% events of each type are shown.

6. Quenching Factor

It is well known for numerous crystal scintillators ($CaWO_4$ [33], $ZnWO_4$ [34], $CdWO_4$ [3], Li_2MoO_4 [35], etc.) that alpha particles induce a lower intensity scintillation signal than gamma quanta of the same energy. Such feature of scintillation pulses could be explained qualitatively by the "Birks law" [36]. One could also consider article [37], wherein a phenomenological model based on "Birks law" is used to interpolate/evaluate such behavior for any charged particle in certain crystal scintillators. This phenomenon is characterized by a QF that shows how the scintillator reacts on different type of particles, and in our case could be defined as the ratio of alpha peak position in an energy scale determined using gamma lines of known energy, to the real energy of incident alpha particles. Thus, the QF is an important characteristic of scintillation detectors, since knowing this parameter one can interpret the collected spectrum and determine a real position of any alpha peak within energy spectrum typically calibrated using gamma quanta. Traditionally, this energy, corresponding to alpha peak position is given in electron-equivalent-energies (e.g., MeVee). A 1 MeV beta/gamma produces 1 MeVee of electron induced scintillation light.

For the first time, the QF for alpha particles with CHC crystal was measured in [15], where an external collimated ^{241}Am alpha source (the real energy of alpha particles after traveling through the collimator was measured to be 4 MeV) was irradiating the CHC crystal the flat side, opposite to the PMT. With the gamma calibrated detecting set-up, pulse height spectra of collimated ^{241}Am alpha particle source was collected and the energy resolution was found to be about 21% with a peak-centroid value of 1.48 MeVee.

The broadness of alpha peak was attributed to the geometry and condition of the used collimator, to the top-face roughness of the CHC crystal, and possibly due to crystal storage conditions, since before this measurement the crystal was stored for a while in a mineral oil. However, the effect of the crystal storing in a mineral oil should be further investigated, because it might have caused a formation of a dead layer on the crystal surface, and consequently, degrading the crystal scintillation response to alpha particles. Authors attribute all these factors in combination to the loss in energy resolution for alpha particles. The measured QF for external collimated 4 MeV alpha particles was found to be 0.36.

Later, the quenching factor for alpha particles was studied in detail utilizing an experimental data collected over 2848 h in low-background measurements with 7 g CHC crystal (see Section 10, below) [7]. There, to extract alpha events related to internal alpha peaks from ^{228}Th decay sub-chain from the entire massive of the experimental data, the time-amplitude analysis of delayed-coincidence events was used (see in details [3,7]). According to the result of the selection after time-amplitude analysis, the alpha peaks of ^{224}Ra, ^{220}Rn and ^{216}Po are located at (2260 $\pm$ 200) keV, (2540 $\pm$ 200) keV and (2780 $\pm$ 240) keV in energy scale of the detector calibrated by gamma quanta, respectively. Hence, the QF of the used CHC crystal at the real alpha energies of ^{224}Ra, ^{220}Rn, and ^{216}Po is 0.39 $\pm$ 0.04, 0.40 $\pm$ 0.03 and 0.40 $\pm$ 0.03, respectively.

Figure 3 represents the experimental values of QF obtained with an internal alpha peaks from daughters of ^{232}Th and ^{238}U decay chains and an external ^{241}Am alpha source and the global fit according to phenomenological model proposed in [37]. This Df dependence indicates that the alpha particles produce more than a third of the light amount produced by gamma quanta in CHC crystals in the energy range (1–8) MeV. Important to notice a great agreement between QF values achieved with external and internal alpha particles, and that both measurements were confirmed with a phenomenological model. The CHC crystal demonstrates a quenching factor higher than 0.3 in the entire energy range and, even further, QF is rising at low energies (below 1 MeV) to more than 0.5, which make such scintillating crystals very attractive in the direct DM particles detection through elastic or inelastic scattering on atomic nuclei. In such experiments the typical goal is to detect heavy nuclear recoil after WIMP interaction with detector media with expected energies less than 100 keV. Hence, having a high QF for alpha particles in CHC crystals, this material is also expected to show a high QF for nuclear recoils, but this point is a subject for further investigations.

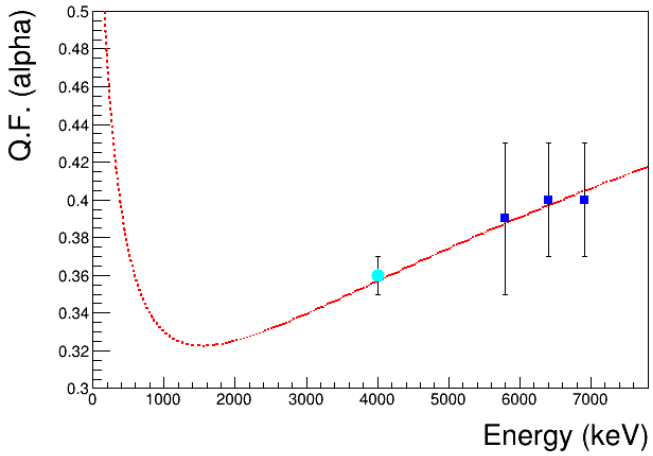

Figure 3. Dependence of the quenching factor (QF) on the energy of alpha particles measured by internal alpha decays of ^{224}Ra, ^{220}Rn, ^{216}Po nuclides in the 7 g CHC crystal (blue squares) [7]. The QF model obtained as a global fit of these data points following the phenomenological model of [37] is also presented (red dotted line). The QF measured with external collimated ^{241}Am alpha source from [15] is also shown (cyan circle).

7. Investigation of the Defect Structure

The scintillation performance of CHC crystals can easily be affected by the presence of lattice and impurity-associated defects. Their own energy states within the band gap can lead to processes biasing the energy transfer toward luminescence centers, e.g., a non-radiative recombination of charge carriers at the lattice defects. Consequently, the luminescence response will degrade and the afterglow can increase. Therefore, knowledge of the defect type, its charge state, local structure, and thermal stability are of great importance in order to proceed with further material improvement.

Because of a hint on the existence of two different V_k centers, one created by the self-trapping of a hole at two regular chlorines forming the Cl^{2-} molecular ion in the Cs_2HfCl_6, and seeking for more details, authors in [38] performed studies by using correlated measurements of EPR, thermo-stimulated luminescence (TSL), and radioluminescence (RL) techniques to evaluate the influence of the material stoichiometry on the irradiation-induced defects, their types, as well as quantity and emission centers.

To do so, the Cs_2HfCl_6 compound was synthesized by the direct reaction of starting cesium chloride (CsCl) and hafnium chloride ($HfCl_4$) powders mixed together in the stoichiometric ratio, and two technological approaches were tested using open and closed systems. In the open system, the CHC compound was purified with gaseous mixture of halogenation agents followed by zone refining. In the closed system, the starting CsCl and $HfCl_4$ were purified separately using the same refinement techniques, and afterwards sealed in the stoichiometric ratio in a quartz ampule under vacuum. The CHC single crystals were grown in vertical furnace with the pulling rate of about 0.5 mm/h and temperature gradient of 40 K/cm under the atmosphere of halogenation agents and vacuum for the open and closed systems, respectively. Samples for optical, TSL, and EPR characterizations were cleaved from the as-grown crystals along the (111) crystalline plane with both facets were mirror polished.

The cylindrical shape of the as-grown Cs_2HfCl_6 crystals, produced in [38], were 12 mm in diameter and (40−55) mm in length depending on the starting charge of the material. The biggest issue with produced CHC1 crystal was the stoichiometry change along the crystal axis reaching the content of 97 mol% of the Cs_2HfCl_6 phase at the start of the crystal and only 22 mol% at the end. In contrast, higher uniformity was achieved in the CHC2 crystal, with 100 and 93 mol% of the Cs_2HfCl_6 phase content along its axis. The CHC3 crystal possessed an excellent uniformity, being 100 mol% of the Cs_2HfCl_6 phase over the whole ingot. Second phase identified in the crystals was CsCl. No other phases were present. Samples for subsequent characterizations were selected from the start of the obtained ingots with the highest Cs_2HfCl_6 phase content. The size of the specimens cleaved and polished from the as-grown crystals was approximately $2 \times 2 \times 1$ mm^3.

Spectrally resolved TSL, EPR and RL methods have been combined in a powerful tool to study the mechanism of charge trapping and its nature in Cs_2HfCl_6 single crystals. Two different EPR signals of V_k centers (Cl_2^- molecular ions, V_k(a) and V_k'(b)) were detected in the CHC crystals and the creation of such types of defects was supposed to be the intrinsic property of the CHC material. The V_k(a) and V_k'(b) trap depths, E_{t1} = (0.11 ± 0.03) eV and E_{t2} = (0.30 ± 0.03) eV, and frequency factors, $f_{01} \approx 10^{2-3}$ s^{-1} and $f_{02} \approx 10^6$ s^{-1}, respectively, were determined from the fit of the EPR signal decay curves. For the V_k(b), the following parameters were obtained: E_{t3} = (0.43 ± 0.03) eV and $f_{03} \approx 10^5$ s^{-1} in a similar way. The strong dependence of the charge carrier trapping processes on the CHC crystal stoichiometry was concluded.

TSL spectra of CHC crystals were very complex, featuring a multicomponent structure within the (10−500) K temperature range. They could be decomposed to up to 2−3 single contributions. Their temperature evolution enabled to distinguish at least two main luminescence mechanisms attributed to Hf and Zr impurity based emissions. Despite the glow curves manifested eight peaks with first-order recombination kinetics, the trap depths and frequency factors could be determined only for the 52, 122, 231, and 288 K peaks. After detailed analysis, the V_k(a) center (hole-like) was expected to be a part of the

self-trapped exciton of the $Hf^{3+}-Cl^{2-}$ form. While nature of the V_k'(b) center is still to be clarified in further studies. Furthermore, based on results of RL, TSL and EPR combined measurements, authors from [39] came to the conclusion that better stoichiometry leads to simultaneous reduction of the number of both the emission centers (Hf- and Zr-based), as well as the trapping centers.

In order to study of the temperature dependence of the luminescence characteristics (before this publication only room-temperature studies on CHC were addressed) and to precisely determine of the emission and trapping centers, the same research group has applied the time-resolved luminescence spectroscopy and EPR techniques in a broad temperature range [39]. Authors synthesized a CHC compound following the procedure as described in [38], while the finally synthesized material was subsequently purified by a combination of gaseous halogenation agents introduced into its melt and zone-melting technique. Then powder was sealed and subjected to the crystal growth at the pulling rate of 0.3 to 0.4 mm/h and temperature gradient of about 40 K/cm. As-grown crystal had 12 mm diameter and 40 mm in length. The samples were cleaved from the grown crystals along the (111) plane with dimensions of $4 \times 4 \times 3$ mm^3 for optical characterizations. No cutting or polishing of specimens was required. Few optical parameters were measured before EPR characterization. First, given the position of the photoluminescence peak the band gap value was calculated to be about 6.3 eV. In addition, the CHC crystal exhibited a wide transmission range, extending from ultraviolet to middle infrared region: about 245 to 2500 nm at room temperature. Then, photoluminescence spectra and decay kinetics were measured in the extended temperature range of (8−500) K and approximated by a phenomenological three excited-state level model. Self-trapped exciton and defect-related emissions were clearly distinguished with the onset of thermal quenching above room temperature. The EPR experiment revealed the formation of two configurations of V_k center (Cl^{2-} molecular ion) at temperatures below (55−60) K. One of the V_k centers is created by a hole self-trapping at two neighboring Cl^- ions. In the temperature range (70−80) K, this state is thermally disintegrated and reappears in another configuration, formed most probably by an interstitial Cl^- ion (an analog of the H-type center in alkali halides). No electron centers were detected in this study.

Further investigations of the defect structure of CHC-family crystals are expected to appear in the near future and it would be beneficial to include into such complex analysis a study on real concentration of impurities measured by mass-spectroscopy technique. This will help to achieve a better understanding of processes occurring in the crystalline media.

8. Chemical Purity

While one could see wide variety of the raw materials purity grade used in crystals production, different purification approaches and noticeable modifications in the growth and thermal conditions, there is no information about actual impurities level either in raw materials or in final crystals. Moreover, no detail information one could find on re-distribution of impurities within the entire crystal production chain. The first and only measurements of a wide list of impurities and their re-distribution due to purification through the three-fold sublimation and CHC crystal growth were reported in [40].

CsCl beads (99.998%) and $HfCl_4$ powder (99.8%) were used as starting materials in this study. Original $HfCl_4$ powder underwent of three-fold static sublimation purification to reduce the concentration of low-vapor pressure impurities. Thereby, 50 g of $HfCl_4$ material were loaded into a quartz ampule, sealed under vacuum, and then placed into a horizontal furnace in a way that the refined $HfCl_4$ material collects in the cold part of the ampule, which stays at room temperature. Each purification stage was performed at a temperature of 400 °C for 12 h. After the third stage, the fraction of purified material was not less than 80% of the initially loaded mass. In order to synthesize Cs_2HfCl_6 charge, the stoichiometric mixture of purified $HfCl_4$ powder and as-received CsCl beads was sealed under vacuum. The synthesis was carried out by gradually increasing temperature up to melting point (820 °C), with the total duration of homogenization and synthesis of about

10 h. Then, the synthesized CHC compound was smashed into small pieces, sealed in new quartz ampule under vacuum and transferred to a two-zone vertical furnace for crystal growth with crystallization rate of (0.5–1.0) cm/day and a temperature gradient of 5 °C/cm at the solid/liquid interface. At the end, the chemical purity of the CsCl, $HfCl_4$ (initial and after purification), and as-grown CHC crystal, i.e., the entire technological chain of the CHC crystal production, have been analyzed with the help of high resolution inductively coupled plasma-mass spectrometer (HR-ICP-MS).

It should be highlighted that HR-ICP-MS measurements of some elements have been unfortunately affected by isobaric inferences of Hf isotopes and its oxides, leading to the high detection limit, when analyzing Hf-containing materials. The most notable interferences were for Yb, Lu, Ta, W, Ir, Pt, and Bi elements, thus this aspect should be taken into account when planning careful concentration determination of these contaminants in the future. Next, it was shown that the proposed three-fold sublimation purification of $HfCl_4$ powder is effective at reducing the concentration of only certain elements. For example, the lanthanum concentration was reduced by about five times (from 2.6 ppm to 0.6 ppm), such elements as K, Mn, Fe, and Sn were reduced by a factor of 3–4, whereas uranium was reduced by a factor of 12 (from 3.20 ppm to 0.27 ppm). Although the concentration of Zr appears not to be affected by this purification treatment on $HfCl_4$ (about 950 ppm), the crystal growth reduced the Zr concentration to below than 100 ppm. Therefore, either additional purification stages should be applied to reduce of the Zr concentration, or a modified purification method should be developed and implemented. Again, the most effective purification occurred during the CHC crystal growth, resulting in a final level of overall contamination of less than 3 ppm for all analyzed elements, excluding Zr (80 ppm). The purity level of CsCl component shows the overall contamination less than 1 ppm for all analyzed elements, thus chemical purity grade 99.998% is sufficient for high quality crystal production, and main attention should be dedicated to purification of the $HfCl_4$ powder.

While the authors of almost all presented articles agreed that high purity raw materials constitute a key parameter to obtain high-quality CHC-family crystals with a high performance as a scintillating detector, there are mainly qualitative expressions regarding this point. We still lack a detailed analysis which will focus on defining a list of critical impurities and an acceptable level of their concentration, which will still not degrade the quality of CHC crystals. Thus, further quantitative studies on the chemical purity of the raw materials, efficiency of purification methods and crystal growth thermal conditions are required.

9. Internal Radioactive Background

The first investigation on the radioactive contamination of raw materials, materials after purification (three-fold sublimation) and the final Cs_2HfCl_6 (CHC) crystals were carried out within 2017 using an ultra-low background high purity germanium (HPGe) detector and presented in [40]. Material samples in plastic bags were directly placed above the end-cap of the HPGe gamma-spectrometer and counted for at least two weeks for each sample. The HPGe detector was installed inside a massive passive shield that consists of low radioactivity lead (25 cm), high purity copper (5 cm), and, in the inner-most part, archaeological lead (2.5 cm). The whole set-up was contained inside a Plexiglas box and continuously flushed by high purity nitrogen gas to exclude the environmental air (see Figure 4). Moreover, the experiment was carried out in Gran Sasso Underground Laboratory (Assergi, Italy) that provided more than 3600 m w.e. of overburden and reduction of muon flux by a factor 10^6.

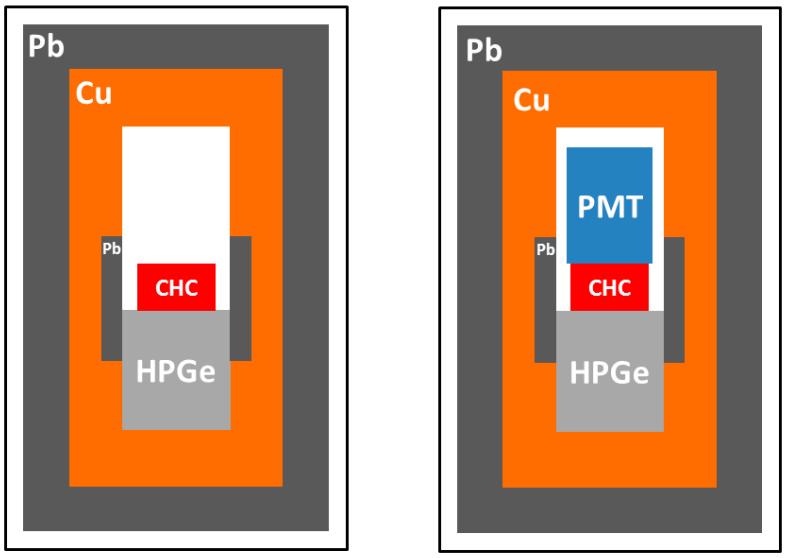

Figure 4. Left: Schematic cross-section view of the low-background experimental set-up with HPGe detector (not in scale) used for measurements of the radioactive contamination of raw materials, materials after purification and the final CHC crystals. Right: Adaptation of the same experimental set-up with HPGe detector for ^{174}Hf rare alpha decay measurements in a coincidence with scintillation channel (PMT). See more description in the text (Sections 9 and 10).

The results of the screening of the as-received CsCl (99.998%) beads, initial $HfCl_4$ (99.8%) powder, the $HfCl_4$ powder after purification by three-fold sublimation, and as-grown CHC crystal are listed in Table 6. From presented results, one could immediately notice that $HfCl_4$ powder is substantially contaminated by radionuclides from ^{232}Th and ^{238}U natural decay chains with activities at the level of (50–130) Bq/kg. The next important point is that secular equilibrium is broken in these natural decay chains, most probably during initial $HfCl_4$ (99.8%) compound production and preliminary purification at production site. Further purification by three-fold sublimation in vacuum leads to redistribution of radionuclide activities, while not reducing their total activity. This issue should be addressed in further dedicated studies.

Despite a high internal radioactivity of starting materials, namely $HfCl_4$ powder, there is no evidence of radionuclides from the natural decay chains of ^{235}U, ^{238}U and ^{232}Th in both analyzed CHC crystals, thus only corresponding limits have been set at a level of a few mBq/kg. At the same time, the data listed in Table 6 exhibit that raw materials for the crystal production play a critical role in the final radioactive contamination of CHC crystals. For example, the contamination of CsCl (99.998%) compound by ^{137}Cs/^{134}Cs artificial nuclides are directly correlated with the activity levels of both isotopes found in CHC crystals, and demonstrates that there is no possibility for purification for those during crystal growth. Moreover, since ^{134}Cs and ^{137}Cs are rather long-living nuclides with half-lives of 2.07 y and 30.08 y, respectively, waiting for a reduction of their activities via decay during the preliminary storage underground it is not a viable solution. Therefore, to produce CHC crystals for future low-background experiments aiming to search for rare nuclear decays, it necessary to carefully check the initial CsCl compound prior crystal growth and to find a supplier that provides material with a minimal amount of ^{137}Cs/^{134}Cs radioactive isotopes. As an alternative solution, one could consider the substitution of Cs by Li or Tl. However, this point should be further studied and dedicated measurements of a market available LiCl and TlCl compounds. In addition, it should be stressed that internal radioactive contamination of the CsCl compound by ^{137}Cs/^{134}Cs artificial nuclides does not depend on the chemical purity grade, but is caused by Cs metal origin, the contamination of used lab ware (equipment), and chemicals involved in the CsCl production chain.

Table 6. The internal radioactive contamination. Activities of radioactive nuclides determined for the entire production chain of Cs_2HfCl_6 (CHC) crystal #1 (as-received CsCl, initial $HfCl_4$ powder, $HfCl_4$ powder after 3-fold sublimation, as-grown CHC crystal #1) and the CHC crystal #2 were measured with low-background HPGe gamma-spectrometer. Activities listed in the last column (CHC crystal #2*) were evaluated from selected by pulse shape analysis "pure" alpha events spectrum collected over 2848 h in long-term low-background measurements of CHC crystal in scintillating mode (see text). All limits are at 90% C.L. N.A. means "not analyzed".

Chain	Nuclide	Activity					
		CsCl	$HfCl_4$	$HfCl_4$	CHC #1	CHC #2	CHC #2*
		Bq/kg	Bq/kg	Bq/kg	mBq/kg	mBq/kg	mBq/kg
^{232}Th	^{232}Th	N.A.	N.A.	N.A.	N.A.	N.A.	0.2 ± 0.1
	^{228}Ra	<0.98	<1.1	<6.3	<12	<12	N.A.
	^{228}Th	<0.82	0.8 ± 0.4	<4.5	<6.3	<3.6	0.2 ± 0.1
^{238}U	^{238}U	N.A.	N.A.	N.A.	N.A.	N.A.	0.6 ± 0.1
	^{234}Th	<22	<58	130 ± 30	<8.6	<0.80	N.A.
	^{234m}Pa	<19	50 ± 20	<140	<3.7	<0.48	N.A.
	^{234}U + ^{230}Th	N.A.	N.A.	N.A.	N.A.	N.A.	1.4 ± 0.2
	^{226}Ra	<0.54	<0.86	<4.5	<12	<23	0.2 ± 0.1
	^{210}Po	N.A.	N.A.	N.A.	N.A.	N.A.	1.4 ± 0.2
^{235}U	^{235}U	<0.53	1.4 ± 0.8	<2.7	<26	<14	N.A.
	^{40}K	<1.6	<2	<8	<0.18	400 ± 100	N.A.
	^{60}Co	N.A.	N.A.	N.A.	<19	<25	N.A.
	^{132}Cs	<0.45	N.A.	N.A.	25 ± 8	<15	N.A.
	^{134}Cs	0.13 ± 0.08	N.A.	N.A.	52 ± 6	79 ± 8	N.A.
	^{137}Cs	1.2 ± 0.2	<0.38	<1.5	830 ± 90	740 ± 90	N.A.
	^{181}Hf	N.A.	<3.1	<1.1	14 ± 0.7	<11	N.A.

Another two observed isotopes, ^{132}Cs and ^{181}Hf, are also not naturally occurring. Both are produced by cosmic ray activation on naturally occurring Cs and Hf isotopes and have relatively short half-lives (6.48 d and 42.39 d, respectively), making them not problematic for exploring rare decays occurring in Hf isotopes. Moreover, to reduce the contamination of the cosmogenic nuclides one should avoid the transportation of the initial materials and finally produced CHC crystals by airplane. As one can see from data listed in the Table 6, for the CHC crystal #2 that was stored for more than one year underground prior the measurements, only limits were set on activities of these isotopes at the level of 15 mBq/kg and 11 mBq/kg, correspondingly. While, CHC crystal #1 that was measured right after transportation by airplane, demonstrates ^{132}Cs and ^{181}Hf contamination at the level of (25 ± 8) mBq/kg and (14 ± 0.7) mBq/kg, respectively. Finally, one would suggest storing produced CHC crystals underground for several months prior starting any low-background experiment that will help to rid both short-lived cosmogenic isotopes.

Surprisingly, but in the contrast to the CHC crystal #1, in the CHC crystal #2, significant activities of ^{40}K at the level of (0.4 ± 0.1) Bq/kg and ^{44}Ti with activity of (10 ± 4) mBq/kg were observed. These radionuclides were not observed in earlier measurements in raw materials, neither in the CHC crystal #1 and further studies of their origin are required. One could speculate that such contamination was originated by a long-term storage of the crystal in different labs, humidity absorption, or by not proper crystal handling prior measurements. The last column of the Table 6 represents activities of daughters' nuclides from ^{238}U and ^{232}Th natural decay chains calculated from the selected "pure" alpha events spectrum, which has been collected over 2848 h in long-term low-background measurements of CHC crystal #2 in scintillating mode (see Section 10 for the description of set-up). The total internal alpha activity in the CHC crystal #2 was calculated at the level of (7.8 ± 0.3) mBq/kg, considering all the alpha events in the selected pulse shape analysis as "pure" alpha events spectrum in the energy range from 0 to 8 MeV.

10. First Observation of Rare Nuclear Processes in Hf Isotopes with Cs_2HfCl_6 Crystal

To produce the CHC crystal sample used in these studies [7], authors utilized raw materials of the same purity grade, applied the purification method by 3-fold sublimation and growth procedures as described in [15,40]. The CHC crystal sample with a mass of 6.9 g, 22 mm in diameter and 4.6 mm height was cut, polished, and then used as a scintillating detector. Crystal was directly coupled to 3" ultra-low-background PMT and placed above the end-cap of the low-background HPGe gamma-spectrometer described above, in Section 9 (see also Figure 4, right). The idea is to use the coincidence between the CHC scintillation detector and the HPGe detector, to study alpha decay of Hf isotopes to the first excited level of daughter nuclides. In this case, when de-excitation gamma quanta are emitted, they will escape the CHC crystal with high probability due to low CHC crystal mass and its density, while they will be more likely to be registered by a large volume HPGe detector located nearby.

The calibration measurements of the CHC crystal as a scintillation detector showed not so exciting results regarding the energy resolution—just 9.1% (FWHM) at 662 keV gamma-line of ^{137}Cs source. However, it still demonstrates an excellent pulse shape discrimination ability using mean-time method that allow to fully separate alpha particles and gamma quanta in the energy interval (0.4–3.0) MeV. Through the pulse shape discrimination and carefully performed the time-amplitude analysis of the entire background data, authors manage to select peaks of internal alpha active nuclides from ^{238}U and ^{232}Th natural decay chains, to determine their activities and corresponding Quenching Factors. The combination of all these parameters provides a complete description of the background model for the selected alpha events. The total internal alpha activity was calculated to be (7.8 $\pm$ 0.3) mBq/kg, considering all the alpha events in the selected "pure" alpha events spectrum in the energy range from 0 to 8 MeV (see Figure 5).

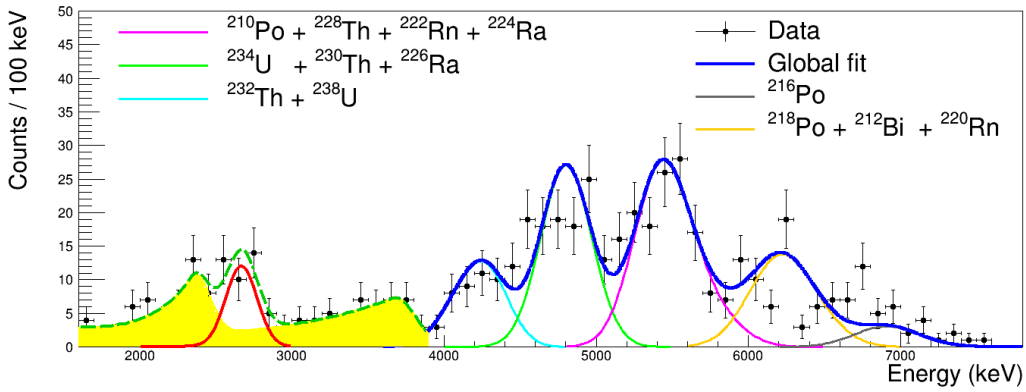

Figure 5. Energy spectrum of the "pure" alpha selected by pulse shape analysis events in the energy range from 1.5 to 8.0 MeV from the data collected in the low-background measurements with the 7 g CHC scintillating crystal over 2848 h [7]. The energy scale is calibrated taking into account quenching factor values for internal alpha particles. Above 4 MeV, the global fit of the data by the background model built based on alpha decays of radionuclides from ^{232}Th and ^{238}U decay chains is shown by blue solid line (individual components of the background model are also shown). Below 4 MeV, the fit of the data with model built from ^{174}Hf alpha decay (red line) and ^{147}Sm alpha decay plus degraded alphas and an exponential function (to describe residual of beta/gamma events) is shown (green dashed line). The yellow area represents the background model with respect to the signal from ^{174}Hf alpha decay.

The experiment to study the rare alpha decay of naturally occurring hafnium isotopes to the ground state and the first excited state using a CHC crystal scintillator in coincidence with an HPGe detector has been completed after 2848 h of live time. The fit of the selected pure alpha events in the energy interval (1.1–3.9) MeV provides the area of the searched peak equal to (31.7 $\pm$ 5.6) events at the expected energy. After a detailed

analysis of all possible interferences to the effect, authors concluded that the rare alpha decay of natural ^{174}Hf isotope was confidently observed with the computed half-life value $T_{1/2} = (7.0 \pm 1.2) \times 10^{16}$ y. This value is in a good agreement with the theoretical predictions and resolves the mystery of the half-life value for this process, which has existed for 50 years. Improved limits were set on rare alpha decay of other natural Hf isotopes to the ground sate and to the first excited state of daughter nuclides at the level of 10^{16}–10^{20} y. Table 7 summarize all obtained results. To improve the experimental sensitivity by more than one order of magnitude compared to the present measurements, one needs to use a larger CHC crystal sample of about 100 g or to increase a number of decaying nuclei via enrichment of Hf isotope of interest, as well as to reduce ^{147}Sm internal contamination by further raw materials purification by a factor 10. All this will allow for the detection of a rare alpha decay of ^{176}Hf isotope and significantly improve limits on other decay modes of natural Hf isotopes.

Table 7. Half-life values of rare alpha decays of natural Hf isotopes measured in [7], in comparison to theoretical estimations (estimations also grabbed from listed in [7]). Natural isotopic abundance (δ) and released energy (Q_α) in these transitions for the g.s. to g.s. decay mode are also listed. All limits are at 90% C.L "N.A." means "not analyzed".

Nuclear Transition	δ, %	Q_α, keV	Final State and Its Energy, keV	Half-Life Value, y	
				Experiment	Theoretical Expectations
^{174}Hf → ^{170}Yb	0.16	2494.5	g.s., 0 1st exc., 84.3	$(7.0 \pm 1.2) \times 10^{16}$ $\geq 1.1 \times 10^{15}$	$(3.5–7.4) \times 10^{16}$ $(0.6–3.0) \times 10^{18}$
^{176}Hf → ^{172}Yb	5.26	2254.2	g.s., 0 1st exc., 78.7	$\geq 9.3 \times 10^{19}$ $\geq 1.8 \times 10^{16}$	$(2.0–6.6) \times 10^{20}$ $(0.5–3.5) \times 10^{22}$
^{177}Hf → ^{173}Yb	18.60	2245.7	g.s., 0 1st exc., 78.6	$\geq 3.2 \times 10^{20}$ $\geq 7.5 \times 10^{16}$	$(0.05–5.2) \times 10^{22}$ $(0.1–120) \times 10^{22}$
^{178}Hf → ^{174}Yb	27.28	2084.4	g.s., 0 1st exc., 76.5	$\geq 5.8 \times 10^{19}$ $\geq 6.9 \times 10^{16}$	$(0.3–1.1) \times 10^{24}$ $(0.7–8.1) \times 10^{25}$
^{179}Hf → ^{175}Yb	13.62	1807.7	g.s., 0 1st exc., 104.5	$\geq 2.5 \times 10^{20}$ $\geq 5.5 \times 10^{17}$	$(0.05–40.0) \times 10^{31}$ $(0.02–25.0) \times 10^{34}$
^{180}Hf → ^{176}Yb	35.08	1287.1	g.s., 0 1st exc., 82.1	N.A. N.A.	$(0.9–57.0) \times 10^{45}$ $(0.2–41.0) \times 10^{49}$

11. Discussion

As one could see from the presented results, within last five years, a large number of articles were published on CHC and CHC-family crystals production, technology variation and its optimization, as well as on characterization of their scintillating performance. Additionally, studies of the crystal defect structure and luminescence centers nature, influence of the variety of doping elements, chemical impurities level, internal radioactive background, and the first confident registration of rare decays that occurs in Hf isotopes have been performed using CHC crystals.

Obviously, CHC and its related compounds are very promising as materials for gamma-spectroscopy, and therefore many groups are attempting to contribute in technology development and ultimate scintillating performance achievement. Despite the fact that one could see a quite random situation with a chemical purity grade of utilized raw materials, mainly for Hf and Zr-based compounds (99–99.9%, no more), as was already mentioned above, and also noticed by some authors, only the highest purity raw materials in combination with highly effective purification methods will allow to obtain the high-quality large volume and crack free CHC crystals. Therefore, detailed studies on raw materials purification methods and conditioning are strongly desired. Moreover, to be able to do more quantitative analysis, and consequently, have a clearer view of the crystal quality driving parameters, efforts made in CHC growth technology development should

be accompanied by raw material characterization by mass-spectrometry at each step of the technological sequence. This could include but is not limited to full characterization of as-received raw materials, materials after purification, the leftover after purification, as-grown CHC crystal, and impurities distribution along the crystal growth axis. Knowledge of present impurities and their concentrations will help to identify and properly assign defects related to undesired impurities or to main luminescent centers, which are responsible for a high scintillating performance of these materials. To date, such mass-spectrometry measurements of initial raw materials, materials after purification and the final CHC crystal were done only once in [40].

One of the main questions that every researcher is interested to answer regarding CHC and CHC-family crystals is—what is the absolute light yield of these crystals and how to reach its maximum? However, currently, no measurements have been performed to determine the absolute light yield. One of the most confident ways to measure it—is to use the light integration sphere. While, values that are presented in all above listed articles, where the peak position under irradiation of known energy gamma-line is comparing to that measured with scintillator of well-defined light yield is the relative light yield measurements, or even to be more correct—the relative light output measurements. Moreover, to correctly estimate the relative light output, one should take into account many experimental parameters that are varying from one crystal to another. For example, light collection efficiency parameter, which is showing how much light is escaped from the crystal and reached PMT window. This strongly depends on the crystal size, its shape and surface treatment, type of the reflector placed around the crystal surface, transmittance of the crystal material to the emitted light, the difference in refractive index of the studied crystal—optical grease—light detector window system, light loses in the optical grease, etc. Without knowing this correction parameter, one cannot compare crystals of different sizes and shapes, since this will introduce a significant error into the calculated value of the relative light output. Another important parameter is the matching spectrum of emitted light and spectral sensitivity of the used light detector. In the best case, it should take into account not only the spectral sensitivity of the light detector at the peaking wavelength, but should be deconvolution of the entire crystal emission spectrum and the entire sensitivity spectrum of the light detector. One important but often omitted experimental parameter is the integration time of the certain set-up and characteristic scintillating time of the standard crystal used for comparison. Since, typically the relative light output is compared to that of the NaI(Tl) scintillating crystal, which has decay time of about 0.25 μs, within the time window of the integration (shaping) time (6–10) μs, its emitted light will be fully collected, while for the CHC crystal, with decay time of about 4 μs, one would need to utilize longer integration time to collect the whole light, otherwise light output will be underestimated. As an alternative solution, one should use a standard scintillator with comparable decay characteristics of scintillating pulses. Therefore, a wide spread of the light output values from different groups, is not only related to the quality of the obtained CHC crystals, but could partially be caused by the above mentioned experimental parameters.

One should also say few words about measurements of the energy resolution under irradiation of high energy gamma sources, like ^{137}Cs. While for a small size samples (less than cm^3), one could easily observe second peak at lower energy, which is corresponded to escaped X-rays of Hf, Tl, Cs or Zr elements from the bulk, with larger samples—the main and escape peaks are merged, thus spreading this cumulative gamma-peak. Hence, there is a logical question: should one describe a gamma-peak as a sum of two Gaussians, or as a single peak at full-absorption energy peak? Depending on your choice, one will get a slightly different FWHM value. Consequently, the energy resolution achieved with your device could be affected by a fitting procedure and not fully represent the quality of the crystal. Thus, this point should be carefully addressed during crystal characterization measurements.

Many questions could occur to careful readers concerning determination of the characteristic decay time components of scintillation pulses. For the sake of quantitative

representation, the scintillation decay curves are often approximated by the sum of several exponential functions: $f(t) = y_0 + \sum_i A_i \exp(-t/\tau_i)$ where y_0 is background, A_i and τ_i are amplitudes and decay time constants, respectively. The scintillation decay curves of CHC samples were fitted using from one to four exponential functions that ensures the best quality of the fit at certain experimental conditions, mainly pulse acquisition time (typically a few tens of μs). However, it should be highlighted that the slow decay time components are essential for the analysis of the final part (tail) of the decay curves, since they would significantly contribute to amplitude of the scintillating pulses, when acquiring in a wide time interval, and consequently, will affect the light output estimation. Moreover, the proper description of scintillating pulse decay components, their actual number and relative amplitudes could be achieved only as a result of a dedicated complex studies involving measurements with TSL and EPR methods, detail photoluminescence analysis under different excitation energies and low-temperature measurements in an optical cryostat, where scintillating signals are recorded over few hundreds of μs, to ensure the full collection of the emitted light. Otherwise, values of the exponential components as a result of the fitting scintillation pulses could be considered only as a preliminary estimation, or as an instrumental characteristic time, demonstrating the fact how kinetics of the light emission in a certain crystal is matching with a shaping tract of the spectrometric unit. Therefore, one could naturally expect a slight variation of decay time values for the same crystal type presented by various groups as a reflection of different chemical purity of raw materials and consequently uncontrolled impurities presence into the crystal (that could lead to slow components contribution enhancement), and by different time intervals of scintillation pulses recording. Further detailed studies on kinetics of scintillation pulses for whole members of CHC-family crystals are strongly desired.

Most characterization measurements with CHC-family crystals were performed under irradiation by gamma quanta, mainly, from a ^{137}Cs gamma source. This is a useful and prompt way how to estimate the general detector performance for gamma-spectroscopy. While only few groups are turning their attention to characterization of the scintillating response of these crystals to alpha particles. More information is needed on energy resolution, quenching factor and pulse shape of scintillating pulses as a function of alpha particles energy. Since alpha particles interact very locally with detector material (in the range of a few to ten μm), while gamma quanta are involving bulk volume through interaction, one could gain a very important information on the difference in excitation energy transfer to luminescence centers at different ionization density, which occur through alpha and gamma events. In addition, the saturation effect at luminescence centers could be studied. Moreover, due to redistribution of the incident energy between decay components of the scintillating pulse for alphas with respect to that for gammas events, it will be possible to study the effect of the involvement of various luminescence centers into the scintillating pulse formation.

As previously mentioned above, with CHC crystals the quenching factor for alpha particles was measured to be about 0.35–0.40 in the energy region of (4–8) MeV, which is a factor of two larger than for any oxide crystals. Based on some phenomenological model, this material could also have an intensive scintillating pulse for nuclear recoil events. However, this assumption should be proved in dedicated measurements with CHC crystal under neutron irradiation. CHC-family crystals could be promising target materials for the direct DM search experiments due to high light output, excellent energy resolution, low energy threshold, expected high quenching factor for nuclear recoils and an ultimate flexibility of crystalline matrix for element substitution. The latter is very important, when considering different models of DM particles with a wide spread of expected masses, hence having an adjustable target material one could match the expected energy of the nuclear recoil, based on kinematics of the DM interaction with regular matter, to energy region with optimal detector performance. As an additional advantage, CHC-family crystals have no directionality of scintillating response due to their cubic crystalline structure. Thus, the energy resolution for alpha particles and nuclear recoils should not depend on the

direction of the interaction with detector, in contrast for example to $CdWO_4$ [3] crystals. It leads to better background discrimination and, as a consequence, to better experimental sensitivity. In light of non-fundamental applications, knowledge of pulse shape and quenching factor will help to design dual-channel detectors, i.e., gamma-neutrons or gamma-alphas spectrometers, which could be useful in homeland security applications.

To provide a fast turn-over with a new type of crystal that related to the CHC-family and facilitate progress in that direction, one should utilize an approach that would allow for a fast test-growth under set of desired changeable conditions (various raw material purity grade, alternative purification procedures, doping with numerous different activators, different thermal conditions and pulling rate, etc.). Recently, such method using the micro-pulling-down apparatus, so-called "miniaturized-vertical-Bridgman" (mVB), was described in detail [41]. The structural and optical quality of the Cs_2HfCl_6 crystal grown within the mVB approach was confirmed to be comparable to the quality of Cs_2HfCl_6 crystals grown by the standard vertical Bridgman method. Hence, authors claim the introduction of a time- and cost-effective method for the single crystal growth that is suitable for a fast screening of A_2MX_6 family compounds.

CHC-family crystals are promising not only as scintillating detectors, but also could have a wide usage in optoelectronic applications. For example, recently the first colloidal synthesis of vacancy-ordered lead-free perovskite Cs_2ZrCl_6 nanocrystals was reported in [42]. The unique vacancy-ordered structure of CZC results in a strongly localized charge-carriers with the formation of self-trapped excitons (STEs). CZC nanocrystals exhibit a high photoluminescence quantum yield of 60.4% at room temperature, with a broadband photoluminescence emission peaked at 446 nm. The emission color can be easily tuned from blue to green by synthesizing the $Cs_2ZrBr_xCl_{(6-x)}$ mixed-halide nanocrystals. In addition, the CZC nanocrystals exhibit a high thermal stability up to 650 °C and long-term air stability for over 6 months. These results suggest that Cs_2ZrCl_6 nanocrystals, and more generally A_2MX_6 family compounds, are promising for optoelectronic applications, and this first study could stimulate future research in the design of new environmentally friendly (Pb-free) nanocrystals.

12. Conclusions

Over the past five years, a new field of an investigation of the recently re-discovered bright scintillating Cs_2HfCl_6 (CHC) and CHC-family materials has emerged and is expanding extensively. Many groups all over the world contribute to these studies. It is very impressive that, in just five years, the long path from a small few mm^3 volume crystal sample with a random quality to a large volume crack-free and high quality CHC crystal with an ultimate scintillating performance has been overcome. Typically, a path of such an extensive R & D stage lasts for about 10–15 years. To date, 25 mm in diameter and about 200 mm long high quality CHC crystalline boule could be produced. A CHC sample with dimensions $\varnothing 23 \times 30$ mm^3 demonstrates 3.2% FWHM at 662 keV, a relative light output at the level of 30,000 ph/MeV, excellent linearity down to 20 keV, excellent pulse shape discrimination ability, and low internal background of less than 1 Bq/kg. Furthermore, attempts to produce a high quality CHC crystal and to reach ultimate performance have prompted studies on this material optimization by the substitution of either alkali ions (Cs to Tl), main element (Hf to Zr), or halogen ions (Cl to Br, I, or their mixture in different ratio), as well as doping the main matrix with various active ions (Te^{4+}, Ce^{3+}, Eu^{3+}, etc.). In the framework of these activities, the brightest red-emission (650 nm) Cs_2HfI_6 scintillator was discovered and demonstrates the relative light output of 64,000 ph/MeV and 4.2% energy resolution at 662 keV. Energy resolution of 3.4% at 662 keV along with the relative light output of 35,000 ph/MeV was measured with a large volume Tl_2ZrCl_6 crystal. Hence, a heavy (Z_{Tl} = 81), relatively fast (about 1.5 μs), bright, and high-quality scintillator is on the way. This has a great importance for high resolution gamma-spectroscopy with advanced sensitivity.

Currently for high sensitivity gamma-spectroscopy, there is a need for scintillators with desired properties, such as high light output, excellent energy resolution, high stopping power (Z_{eff}), fast scintillation decay time, good linearity down to low energies and low cost. Therefore, recent progress in CHC-family crystals production opens up various applications, where such scintillators could be used instead of commonly utilized $LaCl_3$:Ce and $LaBr_3$:Ce crystals. Thus, one should focus on the further production chain optimization aiming the reduction of a general production cost. In this framework, the further improvement of raw materials purification methods, the multi-fold sublimation as one of the most perspective one, along with materials conditioning are required, since only the highest purity raw materials allow to obtain the high quality, large volume, and crack-free crystals.

Another unique feature of CHC-family crystals is the large mass fraction of Hf or Zr elements. In case of Cs_2HfCl_6 and Cs_2ZrCl_6 crystals these mass fractions are 27% and 16%, respectively. Excellent scintillation performance along with a high concentration of nuclei of interest lead to new opportunities for the investigation of rare nuclear processes occurring in Hf or Zr isotopes with a high detection efficiency and subsequently, to advanced experimental sensitivity. For instance, very recently, rare alpha decay of ^{174}Hf isotope with half-life $T_{1/2} = 7 \times 10^{16}$ years was observed with Cs_2HfCl_6 scintillating crystal.

While the main focus within past five years was to achieve large volume and high-quality crystals in a reproducible manner, now is the right time to dedicate more efforts to detailed studies of the material's fundamental properties and understanding variety of the luminescence mechanisms that could occur. The first investigation of the defects structure of CHC crystals showed a great potential of photoluminescence, radioluminescence, electron paramagnetic resonance and thermostimulated luminescence methods in a combination with low-temperature measurements. Therefore, a systematic study of the entire range of CHC-family compounds will shed light on their fundamental properties, and will help to understand the origin of their high light yield and possible paths to further extend it.

To summarize, because of the Cs_2HfCl_6 crystal belongs into a group of compounds with a general formula of A_2MX_6, where A (Li, Na, K, Rb, Cs), M (Hf, Zr, Ti, Pt, Sn, Te) and X(Cl, Br, I), it makes the A_2MX_6 crystalline matrix very flexible. Since each element in the Cs_2HfCl_6 crystal structure can be substituted for an alternative element with an equal ionic charge keeping the structural type unchanged. Therefore, recent progress in the Cs_2HfCl_6 crystal production is only the first step that leads to almost unlimited opportunities in scintillating detector engineering for gamma-spectroscopy with targeted properties. The light output and energy resolution improvement, as well as fine-tuning of the radioluminescence spectrum to match the sensitive region of the used light detector can be achieved by controlled element substitution of the original crystalline matrix.

Funding: This research received no external funding.

Acknowledgments: The author thanks Jonathan Corbett for careful editing of the manuscript and Vincenzo Caracciolo for useful discussions.

Conflicts of Interest: The authors declare no conflict of interest.

References

1. Dolinski, M.J.; Poon, A.W.; Rodejohann, W. Neutrinoless Double-Beta Decay: Status and Prospects. *Ann. Rev. Nucl. Part. Sci.* **2019**, *69*, 219. [CrossRef]
2. Agostini, M.; Araujo, G.R.; Bakalyarov, A.M.; Balata, M.; Barabanov, I.; Baudis, L.; Bauer, C.; Bellotti, E.; Belogurov, S.; Bettini, A.; et al. Final Results of GERDA on the Search for Neutrinoless Double-β Decay (GERDA Collaboration). *Phys. Rev. Lett.* **2020**, *125*, 252502. [CrossRef] [PubMed]
3. Danevich, F.A.; Georgadze, A.S.; Kobychev, V.V.; Nagorny, S.S.; Nikolaiko, A.S.; Ponkratenko, O.A.; Tretyak, V.I.; Zdesenko, S.Y.; Zdesenko, Y.G.; Bizzeti, P.G.; et al. α activity of natural tungsten isotopes. *Phys. Rev. C* **2003**, *67*, 014310. [CrossRef]
4. Belli, P.; Bernabei, R.; Cappella, F.; Cerulli, R.; Dai, C.J.; Danevich, F.A.; D'Angelo, A.; Incicchitti, A.; Kobychev, V.V.; Nagorny, S.S.; et al. Search for α decay of natural Europium. *Nucl. Phys. A* **2007**, *789*, 15–29. [CrossRef]
5. Belli, P.; Bernabei, R.; Danevich, F.A.; Incicchitti, A.; Tretyak, V.I. Experimental searches for rare alpha and beta decays. *Eur. Phys. J. A* **2019**, *55*, 140. [CrossRef]

6. Burger, A.; Rowe, E.; Groza, M.; Figueroa, K.M.; Cherepy, N.J.; Beck, P.R.; Hunter, S.; Payne, S.A. Cesium hafnium chloride: A high light yield, non-hygroscopic cubic crystal scintillator for gamma spectroscopy. *Appl. Phys. Lett.* **2015**, *107*, 143505. [CrossRef]
7. Caracciolo, V.; Nagorny, S.S.; Belli, P.; Bernabei, R.; Cappella, F.; Cerulli, R.; Incicchitti, A.; Laubenstein, M.; Merlo, V.; Nisi, S.; et al. Search for α decay of naturally occurring Hf-nuclides using a Cs_2HfCl_6 scintillator. *Nucl. Phys. A* **2020**, 121941. [CrossRef]
8. Bryan, P.S.; Ferranti, S.A. Luminescence of Cs_2ZrCl_6 and Cs_2HfCl_6. *J. Lumin.* **1984**, *31–32*, 117–119. [CrossRef]
9. Saeki, K.; Fujimoto, Y.; Koshimizu, M.; Yanagida, T.; Asai, K. Comparative study of scintillation properties of Cs_2HfCl_6 and Cs_2ZrCl_6. *Appl. Phys. Express* **2016**, *9*, 042602. [CrossRef]
10. Lam, S.; Guguschev, C.; Burger, A.; Hackett, M.; Motakef, S. Crystal growth and scintillation performance of Cs_2HfCl_6 and $Cs_2HfCl_4Br_2$. *J. Cryst. Growth* **2018**, *483*, 121–124. [CrossRef]
11. Delzer, C.; Zhuravleva, M.; Stand, L.; Melcher, C.; Cherepy, N.; Payne, S.; Sanner, R.; Hayward, J.P. Observations regarding inclusions in the growth of Cs_2HfCl_6 single crystal scintillators. *J. Cryst. Growth* **2020**, *531*, 125336. [CrossRef]
12. Hawrami, R.; Ariesanti, E.; Buliga, V.; Matei, L.; Motakef, S.; Burger, A. Advanced high-performance large diameter Cs_2HfCl_6 (CHC) and mixed halides scintillator. *J. Cryst. Growth* **2020**, *533*, 125473. [CrossRef]
13. Hawrami, R.; Ariesanti, E.; Buliga, V.; Motakef, S.; Burger, A. Latest Progress on Advanced Bridgman Method-Grown K_2PtCl_6 Cubic Structure Scintillator Crystals. *IEEE Trans. Nucl. Sci.* **2020**, *67*, 1020–1026. [CrossRef]
14. Ariesanti, E.; Hawrami, R.; Burger, A.; Motakef, S. Improved growth and scintillation properties of intrinsic, non-hygroscopic scintillator Cs_2HfCl_6. *J. Lumin.* **2020**, *217*, 116784. [CrossRef]
15. Cardenas, C.; Burger, A.; Goodwin, B.; Groza, M.; Laubenstein, M.; Nagorny, S.; Rowe, E. Pulse-shape discrimination with Cs_2HfCl_6 crystal scintillator. *Nucl. Instrum. Methods A* **2017**, *869*, 63. [CrossRef]
16. Rowe, E.; Goodwin, W.B.; Bhattacharya, P.; Cooper, G.; Schley, N.; Groza, M.; Cherepy, N.J.; Payne, S.A.; Burger, A. Preparation, structure and scintillation of cesium hafnium chloride bromide crystals. *J. Cryst. Growth* **2019**, *509*, 124–128. [CrossRef]
17. Kodama, S.; Kurosawa, S.; Fujii, K.; Murakami, T.; Yashima, M.; Pejchal, J.; Kral, R.; Nikl, M.; Yamaji, A.; Yoshino, M.; et al. Single-crystal growth, structure and luminescence properties of $Cs_2HfCl_3Br_3$. *Opt. Mater.* **2020**, *106*, 109942. [CrossRef]
18. Kral, R.; Zemenova, P.; Vanecek, V.; Bystricky, A.; Kohoutkova, M.; Jary, V.; Kodama, S.; Kurosawa, S.; Yokota, Y.; Yoshikawa, A.; et al. Thermal analysis of cesium hafnium chloride using DSC–TG under vacuum, nitrogen atmosphere, and in enclosed system. *J. Therm. Anal. Calorim.* **2020**, *141*, 1101–1107. [CrossRef]
19. Nitsch, K.; Cihlar, A.; Rodova, M. Molten state and supercooling of lead halides. *J. Cryst Growth.* **2004**, *264*, 492–498. [CrossRef]
20. Loyd, M.; Lindsey, A.; Stand, L.; Zhuravleva, M.; Melcher, C.L.; Koschana, M. Tuning the structure of $CsCaI_3$: Eu via substitution of bromine for iodine. *Opt. Mater.* **2017**, *68*, 47–52. [CrossRef]
21. Fujimoto, Y.; Saeki, K.; Nakauchi, D.; Fukada, H.; Yanagida, T.; Kawamoto, H.; Koshimizu, M.; Asai, K. Photoluminescence, photoacoustic, and scintillation properties of Te^{4+}-doped Cs_2HfCl_6 crystals. *Mater. Res. Bull.* **2018**, *105*, 291–295. [CrossRef]
22. Saeki, K.; Fujimoto, Y.; Koshimizu, M.; Nakauchi, D.; Tanaka, H.; Yanagida, T.; Asai, K. Luminescence and scintillation properties of Tl- and Ce-doped Cs_2HfCl_6 crystals. *Jpn. J. Appl. Phys.* **2017**, *56*, 020307. [CrossRef]
23. Kodama, S.; Kurosawa, S.; Yamaji, A.; Pejchal, J.; Kral, R.; Ohashi, Y.; Kamada, K.; Yokota, Y.; Nikl, M.; Yoshikawa, A. Growth and luminescent properties of Ce and Eu doped Cesium Hafnium Iodide single crystalline scintillators. *J. Cryst. Growth* **2018**, *492*, 1–5. [CrossRef]
24. Kodama, S.; Kurosawa, S.; Ohnoa, M.; Yamaji, A.; Yoshinoa, M.; Pejchal, J.; Kral, R.; Ohashi, Y.; Kamada, K.; Yokota, Y.; et al. Development of a novel red-emitting cesium hafnium iodide scintillator. *Radiat. Meas.* **2019**, *124*, 54–58. [CrossRef]
25. Fujimoto, Y.; Saeki, K.; Nakauchi, D.; Yanagida, T.; Koshimizu, M.; Asai, K. New Intrinsic Scintillator with Large Effective Atomic Number: Tl_2HfCl_6 and Tl_2ZrCl_6 Crystals for X-ray and Gamma-ray Detections. *Sens. Mater.* **2018**, *30*, 1577–1583. [CrossRef]
26. Phan, Q.V.; Kim, H.J.; Rooh, G.; Kim, S.H. Tl_2ZrCl_6 crystal: Efficient scintillator for X- and g-ray spectroscopies. *J. Alloys Compd.* **2018**, *766*, 326–330. [CrossRef]
27. Pauling, L. The nature of the chemical bond. IV. The energy of single bonds and the relative electronegativity of atoms. *J. Am. Chem. Soc.* **1932**, *54*, 3570–3582. [CrossRef]
28. Phan, Q.V.; Mohit, T.; Kim, S.H.; Kim, H.J. Crystal growth of a novel and efficient Tl_2HfCl_6 scintillator with improved scintillation characteristics. *CrystEngComm* **2019**, *21*, 5898. [CrossRef]
29. Bhattacharya, P.; Brown, C.; Sosa, C.; Wart, M.; Miller, S.; Brecher, C.; Nagarkar, V.V. Tl_2HfCl_6 and Tl_2ZrCl_6 Intrinsic Scintillators for Gamma Rays and Fast Neutron Detection. *IEEE Trans. Nucl. Sci.* **2020**, *67*. [CrossRef]
30. Hawrami, R.; Ariesanti, E.; Buliga, V.; Burger, A.; Lam, S.; Motakef, S. Tl_2HfCl_6 and Tl_2ZrCl_6: Intrinsic Tl-, Hf-, and Zr-based scintillators. *J. Cryst. Growth* **2020**, *531*, 125316. [CrossRef]
31. Van Loef, E.V.; Ciampi, G.; Shirwadkar, U.; Pandian, L.S.; Shah, K.S. Crystal growth and scintillation properties of Thallium-based halide scintillators. *J. Cryst. Growth* **2020**, *532*, 125438. [CrossRef]
32. Phan, Q.V.; Kim, H.J.; Parka, H.; Rooh, G.; Kim, S.H. Pulse shape discrimination study with Tl_2ZrCl_6 crystal scintillator. *Radiat. Meas.* **2019**, *123*, 83–87. [CrossRef]
33. Zdesenko, Y.G.; Avignone, F.T., III; Brudanin, V.B.; Danevich, F.A.; Nagorny, S.S.; Solsky, I.M.; Tretyak, V.I. Scintillation properties and radioactive contamination $CaWO_4$ crystal scintillators. *Nucl. Instrum. Methods Phys. Rev. Sect. A Accel. Spectrometers Detect. Assoc. Equip.* **2005**, *538*, 657–667. [CrossRef]

34. Danevich, F.A.; Georgadze, A.S.; Kobychev, V.V.; Kropivyansky, B.N.; Nagorny, S.S.; Nikolaiko, A.S.; Tretyak, V.I.; Yurchenko, S.S.; Zdesenko, S.Y.; Zdesenko, Y.G.; et al. Scintillation pulse shape discrimination with $CaWO_4$, $ZnWO_4$, and $CdWO_4$ crystals. *Funct. Mater.* **2005**, *12*, 269–273.
35. Cardani, L.; Casali, N.; Nagorny, S.; Pattavina, L.; Piperno, G.; Barinova, O.P.; Beeman, J.W.; Bellini, F.; Danevich, F.A.; Di Domizio, S.; et al. Development of a Li_2MoO_4 scintillating bolometer for low background physics. *J. Instrum.* **2013**, *8*, 10002. [CrossRef]
36. Birks, J.B. The Theory and Practice of Scintillation Counting. *Proc. Phys. Soc.* **1951**, *A 64*, 874. [CrossRef]
37. Tretyak, V.I. Semi-empirical calculation of quenching factors for scintillators: New results. *Astropart. Phys.* **2010**, *33*, 40. [CrossRef]
38. Kral, R.; Babin, V.; Mihokova, E.; Buryi, M.; Laguta, V.V.; Nitsch, K.; Nikl, M. Luminescence and Charge Trapping in Cs_2HfCl_6 Single Crystals: Optical and Magnetic Resonance Spectroscopy. *Study. J. Phys. Chem. C* **2017**, *121*, 12375–12382. [CrossRef]
39. Buryi, M.; Kral, R.; Babin, V.; Paterek, J.; Vanecek, V.; Veverka, P.; Kohoutkova, M.; Laguta, V.; Fasoli, M.; Villa, I.; et al. Trapping and Recombination Centers in Cesium Hafnium Chloride Single Crystals: EPR and TSL Study. *J. Phys. Chem. C* **2019**, *123*, 19402–19411. [CrossRef]
40. Cardenas, C.; Burger, A.; DiVacri, M.L.; Goodwin, B.; Groza, M.; Laubenstein, M.; Nagorny, S.; Nisi, S.; Rowe, E. Internal contamination of the Cs_2HfCl_6 crystal scintillator. *Nucl. Instrum. Methods A* **2017**, *872*, 23–27. [CrossRef]
41. Vanecek, V.; Kral, R.; Paterek, J.; Babin, V.; Jary, V.; Hybler, J.; Kodama, S.; Kurosawa, S.; Yokota, Y.; Yoshikawa, A.; et al. Modified vertical Bridgman method: Time and cost effective tool for preparation of Cs_2HfCl_6 single crystals. *J. Cryst. Growth* **2020**, *533*, 125479. [CrossRef]
42. Liu, S.; Yang, B.; Chen, J.; Wei, D.; Zheng, D.; Kong, Q.; Deng, W.; Han, K. Efficient Thermally Activated Delayed Fluorescence from All-Inorganic Cesium Zirconium Halide Perovskite Nanocrystals. *Angew. Chem. Int. Ed.* **2020**, *59*, 21925–21929. [CrossRef] [PubMed]